Bio-derived CuO/olive Cake Nanocomposite for Total Phenols Removal from Olive-mill Wastewater

Dilshad Zubair Younis

Submitted to the
Institute of Graduate Studies and Research
in partial fulfillment of the requirements for the degree of

Master of Science
in
Chemistry

Eastern Mediterranean University
July 2016
Gazimağusa, North Cyprus

Approval of the Institute of Graduate Studies and Research

Prof. Dr. Mustafa Tümer
Acting Director

I certify that this thesis satisfies the requirements as a thesis for the degree of Master of Science in Chemistry

Prof. Dr. Mustafa Halilsoy
Chair, Department of Chemistry

We certify that we have read this thesis and that in our opinion it is fully adequate in scope and quality as a thesis for degree of Master of Science in Chemistry.

Dr. Kıvanç Yüney
Co-Supervisor

Assoc. Prof. Dr. Mustafa Gazi
Supervisor

Examining Committee

1. Assoc. Prof. Dr. Mustafa Gazi
2. Asst. Prof. Dr. Şifa Doğan
3. Asst. Prof. Dr. Ozan Gülcan
4. Dr. Akeem Adeyemi Oladipo
5. Dr. Kıvanç Yüney

ABSTRACT

Acutely high organic-loaded olive mill wastewater (OWW) is produced seasonally from the olive oil processing sectors. In North Cyprus, there is no regulated policy regarding the discharge of olive mill wastewater. Hence, the OWW is routinely discharged into the environment top soil or evaporation ponds, and the solid wastes disposed of without treatment to surrounding lands near the processing mills. This poor management of OWW enhances the risk of polluting the surface water and agricultural soil resources.

The environmental threat of the olive mill wastewater is majorly due to the toxicity and low biodegradation of phenolic compounds present in the OWW. This research focused on the feasibility of integrating bio-derived nanoparticles into the surface of waste olives cakes and converting into a high-performance and environmentally nanocomposite adsorbent for removal of total phenol from OWW.

An efficient bio-derived CuO/olive cake nanocomposite (BCO-NC) with 266.11 m^2/g surface area was prepared using banana peel extract. Under optimised conditions (pH 6 and dosage 2.5g), 80% of total phenols was removed after 180 min in the dark (BCO–NC/dark), but rapidly increased to 100% just after 90 min using BCO–NC/H_2O_2/sunlight system at pH 10, dosage 1.0g and H_2O_2 1mM. The removal mechanism is represented by Freundlich isotherm model (R^2= 0.996–1.00) and best modelled by pseudo-second-order kinetic.

Keywords: Bio-derived nanocomposite; olive mill wastewater, total phenols removal

ÖZ

Mevsimsel üretilen zeytinyağı işlemi sırasında, zeytin değirmeni atıksuyu (ZDA) içerisinde fazla mitarda organik madde bulunmaktadır. Kuzey Kıbrıs'ta ZDA deşarj işlemi için herhangi bir politika bulunmamaktadır. Bundan dolayı, ZDA sürekli olarak çevredeki toprağa veya göle boşaltılmakta; pirina - zeytin çekirdeği ve posasından oluşmaktadır- ise zeytinyağı değirmeninin yanında muhafaza edilmektedir, hiçbir arıtma işlemi yapılmadan. Organizasyon zafiyetinden dolayı, ZDA boşaltma işlemi yer üstü ve tarımsal amaçlı kullanılan toprağın kirlenmesine neden olmaktadır.

Zeytin değirmeni atıksuyundaki (ZDA) fenol bileşiklerinin zehir etkisi ve düşük biyoparçalanabilirliğinden dolayı çevreyi tehdit etmektedir. Bu araştırmanın incelediği konu, bio-türetilmiş nano parçaların pirina yüzeyine uygulanması, ve yüksek performanslı ve çevresel nano kompozit adsorban ile ZDA bulunan toplam fenolün uzaklaştırılmasıdır.

Verimli, 266.11 m^2/g yüzey alanına sahip, bio-üretilmiş Cu/pirina nano kompozit (BCO-NK), muz kabukları kullanılarak hazırlandı. En uygun şartlar altında (pH 6ve doz 2.5 g), toplam fenolün %80'i 180 dakika karanlık ortamda (BCO-NK/karanlık) uzaklaştırıldı; fakat pH 10, doz 1.0 g ve 1 m M H_2O_2 şartlarında, BCO-NK/ H_2O_2/güneş ışığı sistemi kullanıldığında, toplam fenol bileşiklerinin %100'ü 90 dakika içerisinde ortamdan uzaklaştırıldı. Uzaklaştırılma mekanizması, Freundlic izoterm modeli ($R^2 = 0.996 – 1.00$) ve en iyi model aldatıcı-ikinci-derece kinetiği.

Anahtar kelimeler: Bio-türetilmiş nano kompozitler, zeytin değirmeni atıksuyu, uzaklaştırılan toplan fenol

DEDICATION

This thesis is dedicated to my Family, most especially my precious dad, Mr. Zubair Younis, who is the pillar that held me throughout my study, to my mum, Mrs. Raqiya Barakat. To my Brothers Faris, Tariq, Azad, Rizgar, Omer, Shaker, Asim and my sisters, thank you and God bless you for your moral, spiritual and financial support, I also would like to appreciate Co-supervisor D. Kıvanç Yüney and Dr Akeem Oladipo who contributed largely to the success of this thesis, God bless you abundantly, to my supervisor, Assoc Prof Mustafa Gazi. God bless and reward you in the folds, you are the best. To all my friends, especially Mohammed Hasan, Salam and Zeyad Qulamany, God bless you all.

ACKNOWLEDGMENT

I will like to thank Associate Professor Mustafa Gazi, Dr. Kıvanç Yüney and Dr Akeem Oladipo who have all contributed to the success of this thesis, for guiding me, teaching and all time tired less support towards the successful completion of my thesis. Thank you all. To my Family who supported my travelling all the way from Kurdistan of Iraq to North Cyprus. May Almighty Allah has always loved, support and be by your side

TABLE OF CONTENTS

LIST OF TABLES

LIST OF FIGURES

Chapter 1

INTRODUCTION

1.1 Background Information

The world olive processing is largely concentrated in the Mediterranean regions, where the biggest olive producers are Greece, Turkey, Spain, Tunisia, Italy, and Albania. Cyprus, as a Mediterranean country, has been ranked recently as among 20th olive oil producer according to the data on International Olive Council (IOC). In Cyprus, olive oil extraction is a popular traditional agricultural practice with an estimated 2.5 million productive trees (Zorpas and Costa 2010). Apart from the Mediterranean countries, the consumption and cultivation of the olive tree are extending to other regions like the Pakistan, Afghanistan, and the United States, African, Asian, and Middle Eastern countries.

Olive mill wastewater (OWW) generated from the olive processing in the Mediterranean region exceeds 30 million annually (Zorpas and Costa 2010). The olive industry generates in addition to olive oil, huge amounts of agro-waste (vegetable waters and spent olives) constituting serious environmental issues. These agro-wastes are unique and increasingly threatening due to the localised and seasonal production, dark coloration, phytotoxic substances (due to phenolic compounds), high and diverse organic content (Anastasiou et al. 2011; Khatib et al. 2009).

Hence, specific management of these by-products with objectives of minimization, treatment, attenuation or valorization of the undesirable environmental impact is necessary. It is not surprising that increasing research efforts are being focussed towards the development of effective treatment technologies (biological and physicochemical processes).

The main management systems of OWW in Cyprus include lagooning as physical evaporation, irrigation for the OWW and subsequent discharge of the residues in soil and/or on landfills (Anastasiou et al. 2011; Zorpas and Costa 2010). Evaporation proffers a good way to minimise the generated liquid waste, but it results in loss of large amounts of water which is limited in Cyprus and simultaneously imparts an odour to the region where such waste is stored.

There are reports regarding the characterization and disposal of olive mill wastewater in southern Cyprus (Anastasiou et al. 2011; Zorpas and Costa 2010). However, to the best of our knowledge, fewer studies report the characterization and negative impact of olive mill wastewater in the northern part of Cyprus. The non-existence of such data for northern Cyprus created environmental and economics threats for the existing olive-oil producers and incoming investors in the region. In an attempt to close this gap, it is extremely paramount to characterise correctly the olive mill wastewater generated in the northern Cyprus and proposes effective treatment technology using wastes generated from the olive mill.

Hence, the main objective of this research is a temporal characterization of olive mill wastewater generated majorly in northern Cyprus. Prepare green nanocomposite from waste olive cakes and apply the fabricated nanocomposite for the treatment of OWW under varying experimental conditions. Data generated from this study is expected to become an indispensable tool in the hands of producers and environmental managers who attempt to administer effective and efficient treatment technologies for the olive mill wastewater generated.

1.2 Extraction Process of Olive Oil from Processing Mills

Globally, Olive fruits have been processed into olive oil which is of health and economic benefits. However, the extraction of olive fruits to produce olive oil generates life-threatening wastes (solid waste, liquid waste and vegetable water), and currently extracted by either the traditional press extraction, 3–phase process or the 2–phase process (Figure 1). In the past years, the common olive oil extraction technique is the traditional press system. Solid wastes known as olive cakes are obtained after the extraction via pressing.

The solid wastes are emulsified using olive oil and then separated by decantation from the remaining olive mill wastewater. These solid wastes are used as animal feed supplements and solid fuels etc. Although the 3–phase extraction process is mostly preferred over the press extraction systems, it utilised higher energy and generates a larger quantity of olive wastes (solids, liquid waste and vegetable water). To reduce the volume of liquid wastes generated in the 3–phase system, the 2– phase process was introduced. The 2–phase process yielded a greater quality olive oil and utilised lower energy; it generates only olive oil and olive mill wastewater regarding waste.

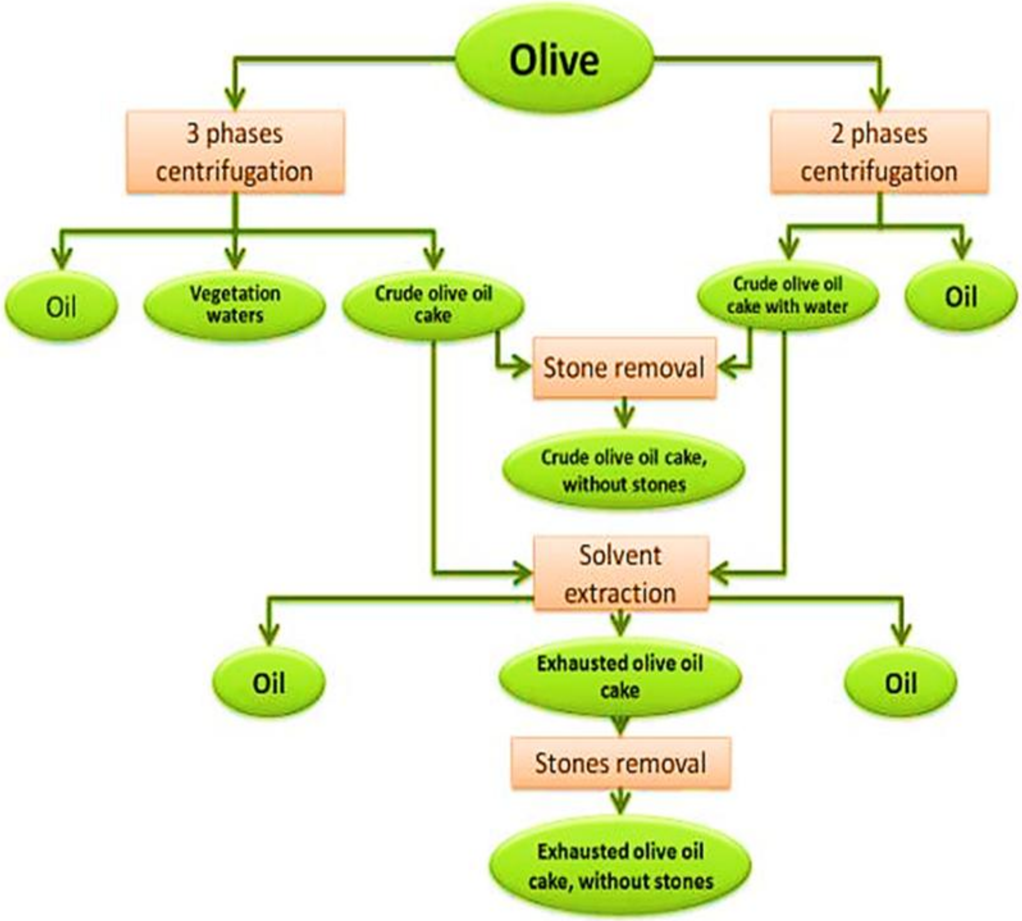

Figure 1: Olive oil processing techniques and products

1.3 General Characterization of Olive Mill Wastes

The olive mill waste is characterised with a distinctive smell, low pH, high turbidity, dark-brownish liquid, high biochemical and chemical oxygen demand (BOD/COD) and high quantity of aromatic-phenolic based compounds. The olive mill wastes are classified as a significant pollutant to the ecosystem due to the presence of large quantity of antimicrobial and phytotoxic substances (i.e., lipids, fatty acids, phenols, etc.) present in the OWW. The chemical composition of the generated vegetable water depends on various factors such as the method of extraction, type of olive fruits extracted and time of maturity of the olive fruits, etc. The chemical compositions of the olive fruits and the vegetable water are presented in Table 1 and 2, respectively.

Table 1: Relative chemical compositions of olive fruits

Components	**Pericarp (%)**	**Olive pulp (%)**	**Stone**	**Total (%)**
Oils	27.3	15.0–30.0	0.70	43.0–58.0
Cellulose	1.90	3.00–6.00	38.0	42.9–45.9
Water	30.0	50.0–60.0	9.10	89.1–99.1
Minerals	1.50	1.00–2.00	4.10	6.6–7.6
Sugar	26.6	3.00–7.50	41.0	70.6–78.1
Polyphenols	0.50–1.00	2.30–3.00	0.10	2.90–3.60
Other compounds	2.40	0.0	3.40	5.80
Organic nitrogen	10.2	2.00–3.00	3.40	15.6–16.6

Source: Niaounakis et al., 2004

Table 2: Chemical compositions of vegetable water from 3-phase

Components	**Percentage composition (%)**
Polyphenols	1.00 – 1.50
Crude protein	1.25 – 2.40
Water	83.0 – 88.0
Fat	0.03 – 1.00
Organic matter	10.5 –15.0
Minerals	1.50 – 2.00

Source: Mebirouk, 2002

The composition of the olive cake obtained after extraction of olive fruits varies largely based on the extraction technique employed. Higher polyphenols had been recorded from the 2-phase extraction system as reported by (Nefzaoui, 1987). The general composition of the olive husk obtained from the three extraction systems is shown in Table 3.

Table 3: Reported characteristics of olive cakes

Components	**3-phase**	**Press system**	**2-phase**
Polyphenols (% w/v)	0.33	1.15	2.43
Moisture (% w/v)	50.2 ± 1.94	27.2 ± 1.05	56.8 ± 2.20
Total sugars (% w/v)	1.05	1.41	1.12
Proteins (% w/v)	3.42	4.81	2.88
C / P ratio	582	614	635
Lignin (% w/v)	10.2	14.2	8.54
Total carbon (% w/v)	29.1	43	25.4
Hemicellulose (% w/v)	7.91	11.2	9.56
Nitrogen (% w/v)	0.52	0.71	0.43
Phosphorus (% w/v)	0.05	0.07	0.04
Calcium (% w/v)	0.44	0.61	0.37
Potassium (% w/v)	0.39	0.54	0.32
Ash (% w/v)	1.7	2.4	1.43
Fats and oils (% w/v)	3.91	8.72	4.65
C / N ratio	57.2	60.6	59.1
Cellulose (% w/v)	17.4	24.1	14.54

Source: Aladham, 2012

1.4 Common Phenolic Compounds in OWW

The phenolic compounds present in OWW possess at least one hydroxyl functional group and an aromatic ring in the backbone. Niaounakis et al. (2004) reported that over thirty polyphenols are present in the olive mill wastewater. Some of the highly abundant polyphenols in OWW are hydroxytyrosol and tyrosol, and some are present in quantitative amounts such as vanillic, cinnamic, *p*-coumaric, ferulic and caffeic acids (Meessen et al., 2001). The combinations of these polyphenols contribute largely to the antibacterial activity and toxicity of the olive mill wastewater, thus, inhibits its microbial biodegradability as reported by Ouzounidou et al., 2008. Some of the abundant phenolics in OWW are depicted structurally in Figure 2.

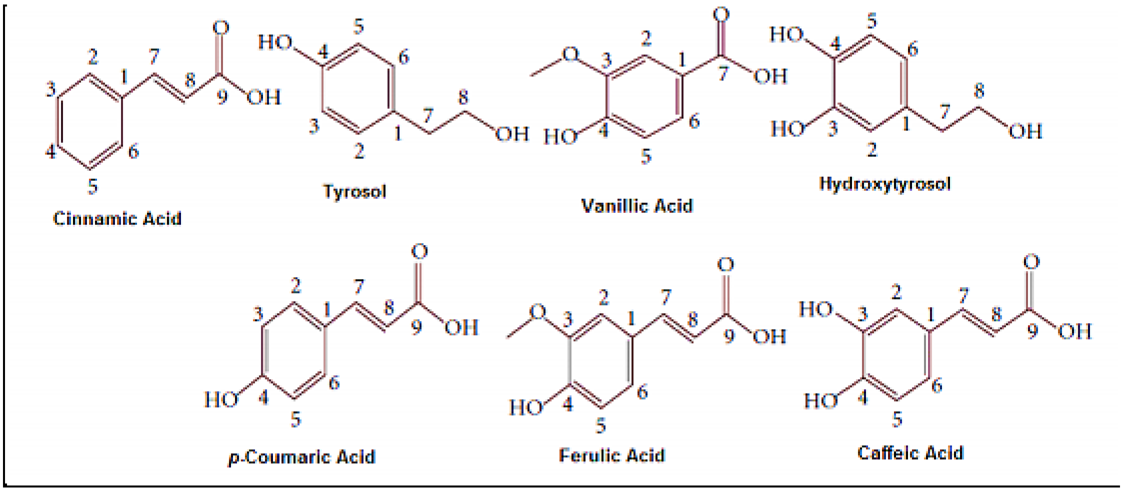

Figure 2: Common polyphenols in OWW (Source: Aladham, 2012)

1.5 Impact of Olive Mill Wastewater in the Environment

Studies have shown that olive mill wastewater is a threat to both the aquatic organisms and the ecosystem in general. These negative effects are mainly due to the high pollution content present in the OWW, its poor biodegradation and adverse toxicity. The environmental impacts are described below:

1.5.1 Impact of Direct Discharge of OWW on Soil

The direct discharge of OWW on soils may destabilise the organism community as a result of the excessive quantity of phenolic compounds present in the olive wastewater (Rousidou et al., 2010). Furthermore, the cation exchangeability of the soil can be inhibited by the presence of significant amount of mineral acids in the OWW; hence, reducing the soil porosity and aggregation properties (Cox et al., 1997). Researchers have reported that direct discharge of OWW onto the soil surface enhances the presence of toxic heavy metals in the environment and (Bejarano and Madrid, 1992). As mentioned, the OWW is characterised by low pH; hence, the acidic nature of the OWW could be extensively corrosive and causes deterioration of the sewer pipes (Niaounakis et al., 2004).

1.5.2 Impact of Direct Discharge of OWW on Aquatic Environment

The toxicity of olive mill wastes on the aquatic ecosystem is alarming and unaesthetic. The brownish-dark colour of the olive mill wastewater has a negative impact on aquatic biota due to inhibition of photosynthesis. The colouring matter is mainly due to the oxidation and subsequent polymerization of tannins (Ntougias et al., 2013). The presence of reducing sugars and phosphates in the olive mill wastewater may lead to the growth of pathogens and eutrophication. As reported by (Obied et al., 2007; Ntougias et al., 2013), the greater the phenolic content of the OW the higher the growth inhibition of aquatic organism. Hence, direct discharge of the olive mill wastewater into aquatic streams will not only result in environmental hazards but also enhance pathogen growth.

1.5.3 Phyto–genotoxicity of OWW on Animals and Plants

The immensely high phenolic content of the OWW hinder causes leaf and fruit abscission and hinders normal plant growth (Della et al., 2001). El-Hajjouji et al., (2007) reported that the hamster embryo cells exposed to phenol or catechol might induce chromosomal aberrations and unscheduled DNA production. Also, catechol has been reported to affect the production of micronucleated cells in lymphocytes and increased the quantity of positive-kinetochore micronuclei (El-Hajjouji et al., 2007).

1.6 Olive Mill Wastewater Treatment Techniques

Various pre-treatment, post-treatment and single complete treatment processes have been reported for the management of olive mill wastewater. Some of these techniques are depicted in Figure 3.

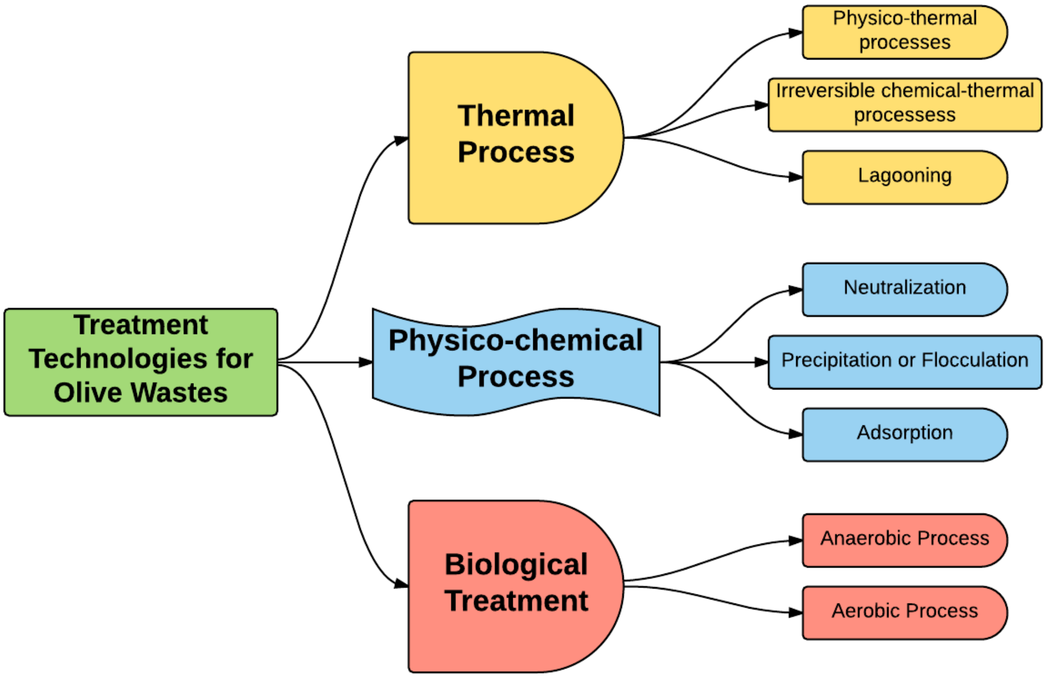

Figure 3: General treatment technologies for olive mill wastewaters

Each treatment process has its advantages and drawbacks. However, adsorption technique has been regarded as a suitable and high-efficient method to treat various pollutant-bearing wastewaters. Adsorption is regarded as a physico-chemical technique involving the transport and attachment of adsorbate (dissolved molecules) within the aqueous medium to the surface of the adsorbent (Oladipo et al., 2015). Some of the advantages of adsorption technique include ease and flexibility, low space requirements, no emissions of odour and wider application in various pollutant-laden wastewaters. However, some adsorbents have been reported to be highly expensive, have low uptake capacity and poor regeneration ability. Hence, the search for low-cost, high-performance adsorbents specifically for treatment of olive mill wastewater is still ongoing.

1.7 Research Goals

As earlier stated, the olive mill wastewaters generated in Cyprus are routinely released into the environment or evaporation ponds, thus resulting in environmental alteration of the immediate ecosystem. Thus, the present research aims to:

I. Monitor and assess the discharge pathway of the olive mill wastewater in northern Cyprus.

II. Collect and characterise samples of the freshly generated olive mill wastewater.

III. Fabricate high-performance adsorbent via ***green approach*** using banana peel and employ the adsorbent for the treatment of the characterised OWW.

IV. Investigate various operating parameters influencing the treatment of OWW and optimise the treatment process to achieve total phenol removal.

V. Investigate the total phenol removal mechanism and sorption rate behaviour using the fabricated nanocomposite.

Chapter 2

EXPERIMENTAL

2.1 Reagents

Analytical grade chemicals and reagents are used in this research without further purification as listed in Table 4.

Table 4: Reagents and manufacturers

S.N	Chemicals and Reagents	Sources
1	Potassium Dichromate	BDH chemicals / England
2	Sulfuric acid (95–97 %)	Sigma–Aldrich/Germany
3	Ferrous ammonium sulphate	BDH chemicals / England
4	Silver sulphate	Riedel-de Haën/Germany
5	Mercury sulphate	Sigma–Aldrich/Germany
6	Ferroin indicator (1,10-Phenanthroline hydrate)	BDH chemicals / England
7	Copper(II) nitrate	Sigma–Aldrich/Germany
8	Hydrogen peroxide (30%)	Merck / Germany
9	Sodium carbonate	Sigma–Aldrich/Germany
10	Folin–Ciocalteu’s phenol reagent	Riedel-de Haën/Germany

2.2 Collection of OWW and Solid Olive Cakes

Three different samples of OWW were obtained from 3-phase olive processing mills located in the Karpaz district of Northern Cyprus towards the end of December 2015. The sample collection was done using a capped 2.0 litres plastic containers, then transported immediately to the Eastern Mediterranean University and stored at a temperature around 5◦C in the polymeric materials research refrigerator. The solid olive cakes were collected from same olive processing mills, thoroughly washed, sieved to powder form and stored for later use.

2.3 Analyses and Sample Characterization

The biochemical oxygen demand (BOD), chemical oxygen demand (COD), total solids (TS), total suspended solids (TSS) of each OWW samples were analyzed following the procedure of the "**Standard Methods for Examination of Water and Wastewater**", in 5210B, 5220 C, 2540 B and 2540 D, respectively (Clescer et al., 1999). The pH, total dissolved solids (TDS), salinity, total organic carbon (TOC), electrical conductivity (EC) and density measurements pH of the collected samples were measured using calibrated Benchtop pH meter (InoLab pH/Cond 720–Gemini BV).

The total phenol content was determined using spectrophotometric method via Folin-Ciocalteau procedure described elsewhere (Stasinakis et al., 2008). Briefly, a 1.5 mL of Folin-Ciocalteu reagent was mixed with 25 mL diluted phenolic standard in the presence of 200 g/L sodium carbonate solution. The mixture was stirred for 30 min at room temperature and left in the dark at 25 ◦C for two hours. Then, the absorbance of the mixture was determined using UV/VIS spectrophotometer (UV-Win 5.0) at 750nm. Before the absorbance reading, the instrumental calibration was performed using varying standard phenol solutions concentrations (0.0–1.0 mg/L). Triplicate analyses were conducted, and average results are tabulated in Table 5.

Table 5: Characteristics data from the three samples of OWW

Parameter	**Sample 1**	**Sample 2**	**Sample 3**
Ph	4.95±0.35	5.01 ±0.49	4.91±0.34
TSS (mg/L)	898±0.77	308±0.88	351±0.66
TOC (mg/L)	8956±0.45	8091±0.67	8789±0.34
Density (kg/m^3)	452±0.33	498±0.89	409±0.11
TS (mg/L)	2651±0.11	2009±0.99	2003±0.61
BOD (mg/L)	5671±0.22	4981±0.78	5786±0.67
TDS (mg/L)	1753±0.64	1701±0.44	1651±0.33
EC (mS/cm)	10.52±0.45	9.91±0.45	10.67±0.78
Total phenols (mg/L)	**654 ± 0.44**	**786 ± 0.43**	**898 ± 0.43**
Salinity	9.7±0.65	10.1±0.67	10.7±0.31
COD (mg/L)	7895±0.23	7556±0.88	7771±0.22

2.4 Adsorbent Preparation (CuO/olive cake nanocomposite)

In the present research, copper oxide nanoparticles were fabricated and integrated on the surface of the olive cake via an efficient and green approach using banana peel through a modified procedure (Tamuly et al., 2014). Specifically, banana peels collected from fruits stores were dried in sunlight for days, and then the dried peels were subjected to heat treatment using a muffle furnace at 500 °C for 2 h to obtain peel ash. 100 ml of distilled water was added to 10 g of the ash and filtered. In a separate reaction flask, 10 g of pre-treated dried olive cake powder was added to 80 ml of 2M $Cu(NO_3)_2 \cdot 3H_2O$ solution and the ash filtrate was added to the mixture and stirred at 80 °C vigorously. After 30 min, a colour change was observed slowly from the initial blue colour to a light green and precipitate was formed. The solution was filtered; the precipitate then subjected to thermal treatment 1 h at 500 °C for the formation of powder CuO/olive cake nanocomposite, cooled in a desiccator and labelled BCO–NC for OWW treatment.

2.5 Characterization of the Adsorbents

The BCO–NC was characterised following the procedures described elsewhere as listed below:

2.5.1 Determination of Percentage Ash Content of BCO–NC

The BCO–NC was weighed accurately into a cleaned capped crucible to obtain 0.5 g sample and then burnt on a Bunsen burner until no smoke was observed. The burnt sample was heated at 600^{o}C in a muffle furnace until it turned grey (ash). The ash was cooled and weighed to a constant weight, and the ash content was calculated according to the following equation:

$$\text{Ash}\,(\%) = \left(\frac{W_a}{W_s}\right) \times 100 \qquad (1)$$

Where W_s represents the initial weight of the BCO–NC and W_a is the final weight obtained from the BCO–NC ash.

2.5.2 Bulk Density Determination for BCO–NC

A pre-washed a graduated container was filled with 10 mL distilled water, dried and re-weighed. Then, the container was filled to the brim by BCO–NC and tapped continuously to obtain a constant weight. The weight of BCO–NC that filled the container was determined as 1.89 g, the bulk density was determined according to the following equation:

$$\text{Bulk density of BCO-NC} = \frac{W_{\text{BCO-NC}}}{\text{Volume of container}} \tag{2}$$

2.5.3 Surface Functional Groups, pHpzc and BET Surface Area

The surface area of BCO–NC was assessed using a laboratory-modified nitrogen sorption-desorption technique and calculated by the BET model equation. The pHpzc of BCO–NC was determined by the plots of the initial versus the final pH of the BCO–NC (Oladipo et al., 2015). Briefly, a certain quantity of BCO–NC was added to conical flasks containing 0.1 M KCl solution (25 mL each). After 24 h agitation, the final pHs of the mixtures was taken, and the pH_{pzc} is the intersection point of the plot of final versus initial pH. The amount of the surface acidic and basic groups of the BCO–NC was measured following the Boehm titration technique as described by Oladipo and Gazi (2015) previous work.

2.5.4 Percentage Yield, Moisture Content and Weight Loss

Accurately weighed raw materials for the fabrication of the BCO–NC was processed as earlier described in section 2.4 and the final product was weighed to constant weight. Then 1.0g of BCO–NC was placed into a pre-weighed crucible. The crucible containing the BCO–NC was kept in a conventional oven for 6 hours at 150^{o}C. The well-dried sample was cooled to room temperature and weighed to obtain a constant weight. The percentage yield, moisture content and the weight loss were calculated according to the following equations respectively:

$$\text{Percentage yield of BCO-NC} = \frac{\text{Final weight of product}}{\text{Weight of raw materials}} \times 100 \tag{3}$$

$$\text{Moisture content (\%)} = \frac{W_{\text{BCO-NC}} - W_{\text{dried}}}{W_{\text{BCO-NC}}} \times 100 \tag{4}$$

$$\text{Weight loss (\%)} = \frac{\text{Weight of raw materials} - \text{Final weight of product}}{\text{Weight of raw materials}} \times 100 \tag{5}$$

2.6 Adsorption Experiments

Initially, the standard solutions for total phenol removal were prepared by serial dilutions and concentration 5–25 mg/L was utilised for the calibration curve. The reproducibility and repeatability of the procedure were high with relative standard deviation less than 9.8%. Preliminary sorption experiments were conducted using the three OWW samples; however, the effect of various parameters and final results in this thesis was focused on sample 3 with the highest phenol content (898 mg/L).

Known quantities of BCO–NC were introduced into 200 mL conical flasks containing OWW of varying concentration of total phenols; the reaction flasks were agitated for a day, and a certain volume of OWW was withdrawn at predetermined time intervals. The treated OWW was filtered, and the total phenols concentrations of the filtrates were determined. For comparison, non-filtered samples were analysed, and blank control experiments were performed using flasks containing only adsorbent and distilled water. Furthermore, batch experiments were performed in flasks containing known total phenol concentration without BCO–NC so as to quantify the possible loss of phenolic compounds to the reaction flasks. The flasks were covered during the reaction to prevent volatilisation of phenolics. The total phenols were investigated at varying BCO–NC concentration (0.5–2.5g); initial total phenol concentration (50–500 mg/L); equilibrium treatment time (30–180 min) and pH (3–12) at 150 rpm.

To investigate the photo-reductive potential of the BCO–NC, the OWW was treated under sunlight to removal the total phenol under various conditions similar to those performed in the dark (laboratory). Here, the influence of hydrogen peroxide on total phenol removal was checked. Duplicate experiments were conducted and after equilibrium time, both filtered and unfiltered samples were analyzed for total phenols removal and the percentage removed was obtained according to:

$$R(\%) = 100 \times \frac{C_0 - C_e}{C_0} \tag{6}$$

Where R(%) is the percentage removal, C_o is the initial concentration of total phenols in the OWW, and C_e is the equilibrium concentration at a certain time.

Chapter 3

RESULTS AND DISCUSSION

3.1 Adsorbent Preparation and Characterization

The adsorbent was successfully fabricated using banana peel as a non-toxic and cheap source of sodium (Na^+), potassium (K^+), chloride (Cl^-) and carbonate ions. The ions act as capping/reducing agents for the formation of nanoparticles. According to the titration result and literature reports, about 1.0 g of banana ash contained 0.24 g of K^+, 0.021 g of Cl^- and 0.002 g of Na^+ (Hazarika et al., 2016; Tamuly et al., 2014). These ions are probably responsible for the transformation of $Cu(OH)_2$ to CuO particles on the surface of the olive cake powder according to the following reaction mechanisms:

$$\mathrm{Cu(NO_3)_2 \cdot 3H_2O + Na^+ \xrightarrow{H_2O} Cu(OH)_2 + CO_2 + NO_3^- Na^+}$$

$$\mathrm{Cu(OH)_2 + Olive\ cake \xrightarrow{500^0 C} CuO/Olive\ cake\ Nanocomposite}$$

The results from the Boehm experiments and pHpzc confirmed that the surface the BCO–NC is basic in nature and exhibited pHpzc at 4.7 and 11.2 as shown in Figure 4. At pH below the pHpzc, the surface of BCO–NC becomes predominately positive while at solution pH above the pHpzc, the surface becomes negatively charged (Ngwabebhoh et al., 2016a). The BCO–NC seems to be less pH sensitive and such character will make the adsorbent suitable for wider range of pH.

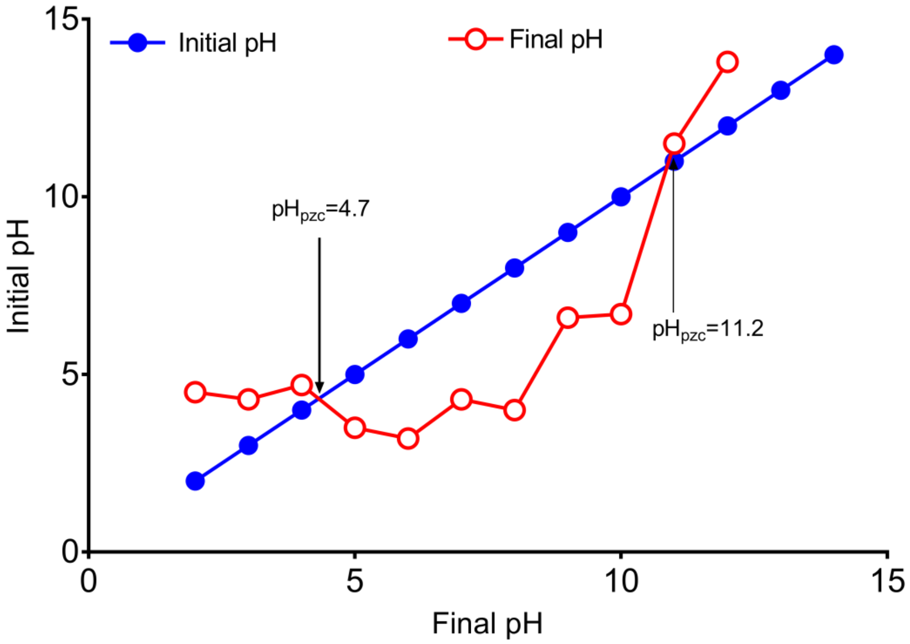

Figure 4: pHpzc determination for BCO–NC

The total basic sites available on BCO–NC were 1.37 meq/g which is higher than the total acidic functional sites (lactonic = 0.37 meq/g, phenolic = 0.23 meq/g, carboxylic = 0.33 meq/g). The detailed characteristics of the BCO–NC are presented in Table 6. The thermogravimetric and differential thermal analyses (TGA–DTA) curves for BCO–NC is depicted in Figure 5.

The TGA measures the weight loss of the BCO–NC as the temperature progresses. The weight loss might be due to the chemical phenomenon (combustion or decomposition) or physical transition such as desorption, evaporation, etc., (Menkiti et al., 2016). The DTA measures the heat emitted or absorbed by BCO–NC, and such heat can be as a result of crystallisation, melting, oxidation or decomposition. The first weight loss of BCO–NC is due to the internal; about 5.5–14.8% weight loss was recorded in the second and third phases at a temperature < 400^{o}C and could be ascribed to decomposition of banana peel extract and cellulosic contents of the BCO–NC.

Table 6: Detailed characteristics of the BCO–NC

Parameters	**Values**
Yield (%)	88.9
Weight loss (%)	11.1
Moisture content (%)	4.68
Specific surface area (m^2/g)	536.55
Ash content (%)	4.12
Bulk density (g/ml)	0.456
pH_{pzc}	4.7 and 11.2
Pore volume (cm^3/g)	0.067

As earlier mentioned, the olive cake consists of lignin, hemicellulose and cellulose, these cellulosic contents decomposed at a temperature lower than 400 ^{o}C. Also, an endothermic reaction occurred at 400 oC which might be attributed to the decomposition of the $Cu(OH)_2$ into CuO (Tamuly et al., 2014). Above 550^{o}C, a significant weight loss (19.7%) occurred which may be due to pyrolysis of the lignin or cellulosic contents of the BCO–NC. The adsorbent remains stable afterwards and 4.56 mg final weight was obtained after the analyses representing about 89.04% of the original BCO–NC weight.

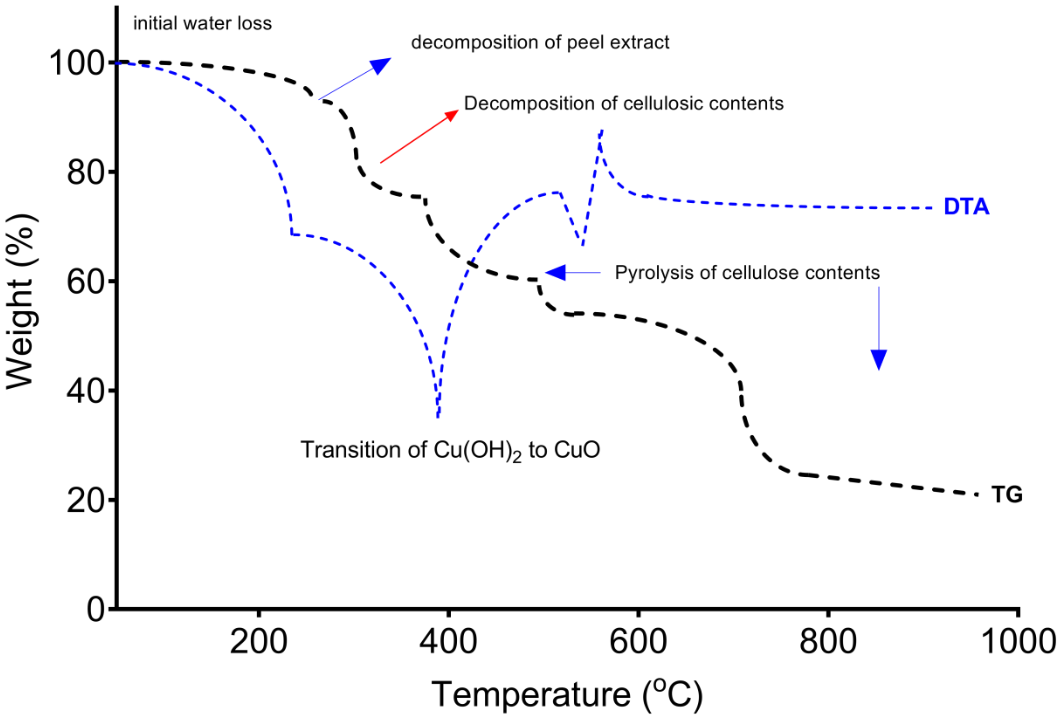

Figure 5: TGA–DTA analyses of BCO–NC

3.2 Influence of Variables Affecting Phenol Removal

The colour and toxicity of the OWW are due to the presence of various phenolic compounds. These polyphenols are recalcitrant in nature; hence, the influence of factors affecting the total phenols removals is described below. The calibration curve for the total phenols is shown in Figure 6, and the percentage phenol removal from the OWW is calculated using equation 6.

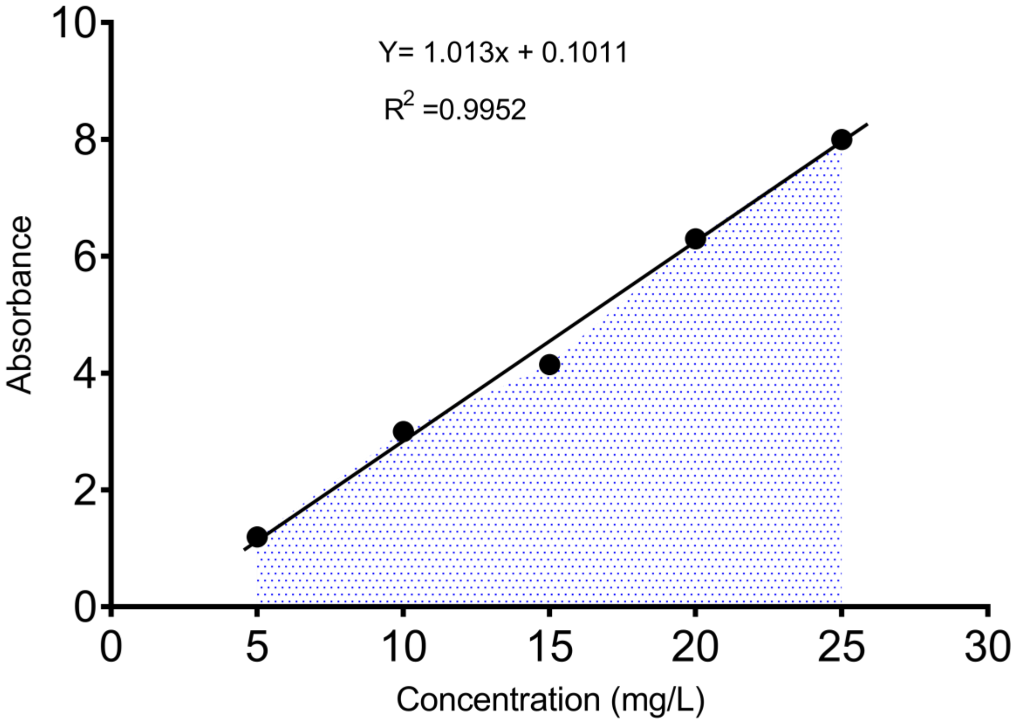

Figure 6: Calibration curve for total phenols

3.2.1 Influence of BCO–NC Concentration

Adsorbent concentration has a significant impact regarding performance and economics of the treatment technology. Hence, the impact of BCO–NC concentration on the removal efficiency of total phenols is depicted in Figure 7. Here, the pH of the solution was not adjusted, and initial total phenols concentration of 800 mg/L was used. Based on the experimental observation, the total phenols removal increased with increasing BCO–NC concentration from 0.5 to 2.5 g/L. Approximately 23% total phenols were removed within 180 min when 0.5 g/L of BCO–NC was used. The removal efficiency exceeded 80% as the BCO–NC concentration increased beyond 1.5g/L.

The increasing trend in the removal efficiency is attributed to increases in the specific surface area of BCO–NC and availability of more sorption sites

(Anandkumar and Mandal, 2012; Nassar et al., 2014). The experimental results confirmed the high sorptive capacity of BCO–NCA as compared with reported treatment techniques. For instance, OWW containing 1470mg/L initial total phenol was left for 90 days in the evaporation pond, but only 43% reduction was recorded (Saez et al., 1992). Similarly, 50% total phenols reduction was reported after one hour of electrolysis for OWW containing 11410mg/L initial phenol concentration (Israilides et al., 1997). Hence, the BCO–NC removal rate outperformed most reported treatment methods.

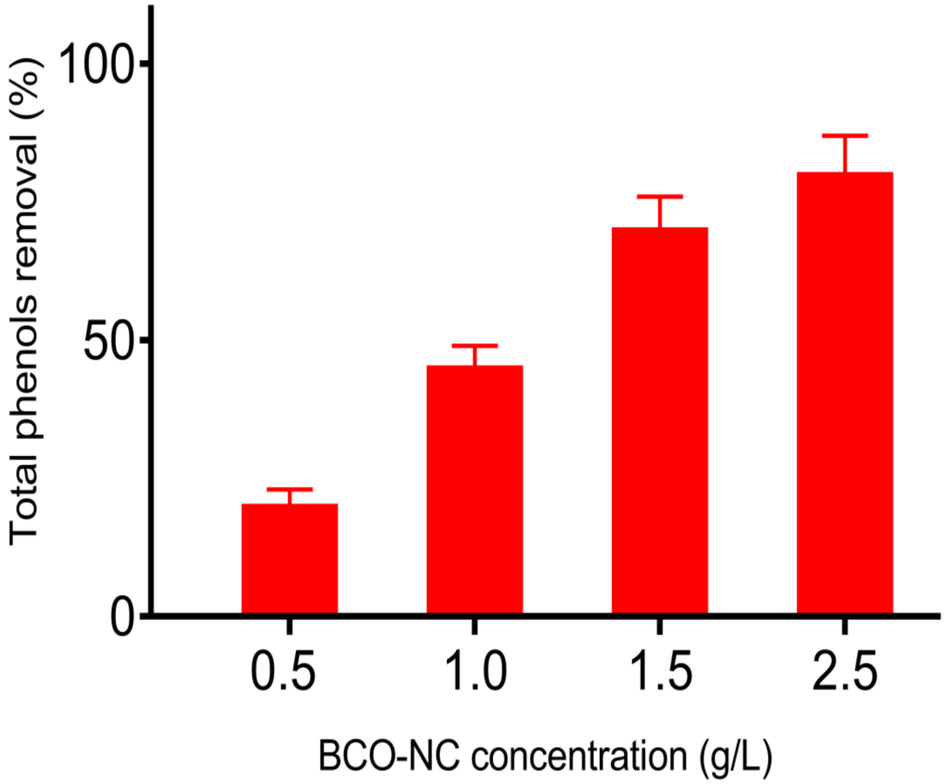

Figure 7: Influence of BCO–NC concentration on the polyphenol removal

3.2.2 Influence of Treatment Time

Control experiments were conducted in the absence of BCO–NC and non-filtered treated sample (in the presence of BCO–NC) to ascertain if the phenols are adsorbed by the flask or the filter paper. Interestingly, total phenols were not adsorbed on the flasks walls and the little quantity adhered to the filter paper was considered during the data analyses. The influence of BCO–NC contact time on total phenols removal was investigated at pH 6 using OWW sample containing 800 mg/L initial total phenols concentration at varying BCO–NC doses.

As presented in Figure 8, total phenols removal by 1.0 g and 2.5 g BCO–NC were high within the first 90 min, the removal percentage of 1.0 g BCO–NC was noticed to reduced slowly beyond 90 min after attainment of 58% total phenol removal. Contrastingly, the 2.5 g BCO–NC gradually decreases until equilibrium was achieved after 120 min and the removal efficiency exceeded 80% after 180 min of the experiment. A similar trend has been noticed during the effect of BCO–NC concentration. The rapid removal during the first 90 min is ascribed to the enhanced migration of the polyphenols to the abundant sorption sites on BCO–NC.

In the first rapid stage, the polyphenol were adsorbed on the external surfaces and large pores of the BCO–NC (Muthusamy et al., 2013). Progressively, the second slow stage involves gradual transport of the phenolic molecules into the smaller micropores of the BCO–NC due to diffusional influences (Stasinakis et al., 2008). At the end of the experiment, the 2.5 g BCO–NC removed about twice the capacity of 1.0 g BCO–NC and could be attributed to earlier consumption of the active sites of the 1.0g BCO–NC.

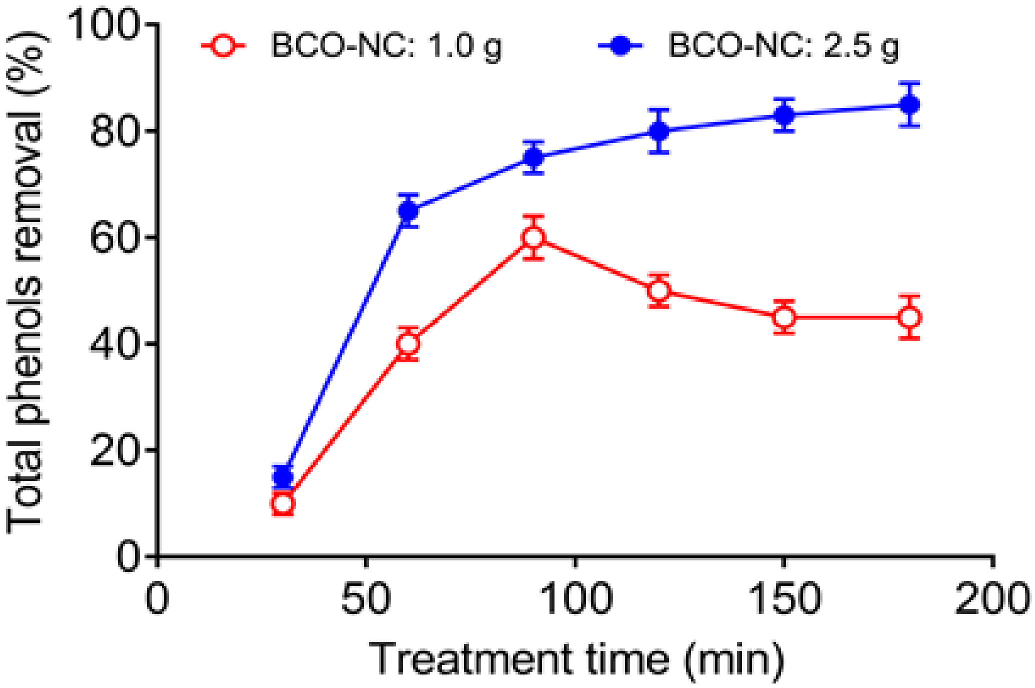

Figure 8: Effect of BCO–NC contact time for polyphenols removal

3.2.3 Influence of Solution pH

The influence of pH on the efficiency of BCO–NC for the removal of total phenols was investigated using series of flasks containing OWW (initial total phenols concentration: 800 mg/L) and 1.0 g BCO–NC at various pH values (3–12). As observed, the BCO–NC removal efficiency for total phenols in the OWW increased with increase in solution pH from pH 3 and higher removal rates were seen at pH 6 and 10 (Figure 9). As known, phenols are undissociated at pH values lower than their p*K*as but dissociate into anionic species at pH higher than the p*K*a, then leaving behind a significant number of neutral molecules (Oladipo et al., 2016).

Here, a definite conclusion cannot be reached on the existence of neutral or ionic forms of the phenolic compounds since the OWW contains a variety of polyphenols with different p*K*a values. The BCO–NC appears to be pH insensitive at a wider range of the OWW pH and this behaviour could be attributed to its two-point pH_{pzc}.

Since the phenol p*K*a is estimated to be 9.89 (Dabrowski et al., 2005) and the BCO–NC pH_{pzc} ranges between 4.7 and 11.2, it is concluded that the polyphenols and BCO–NC surface groups interacted in both deprotonated and protonated forms (Stasinakis et al., 2008).

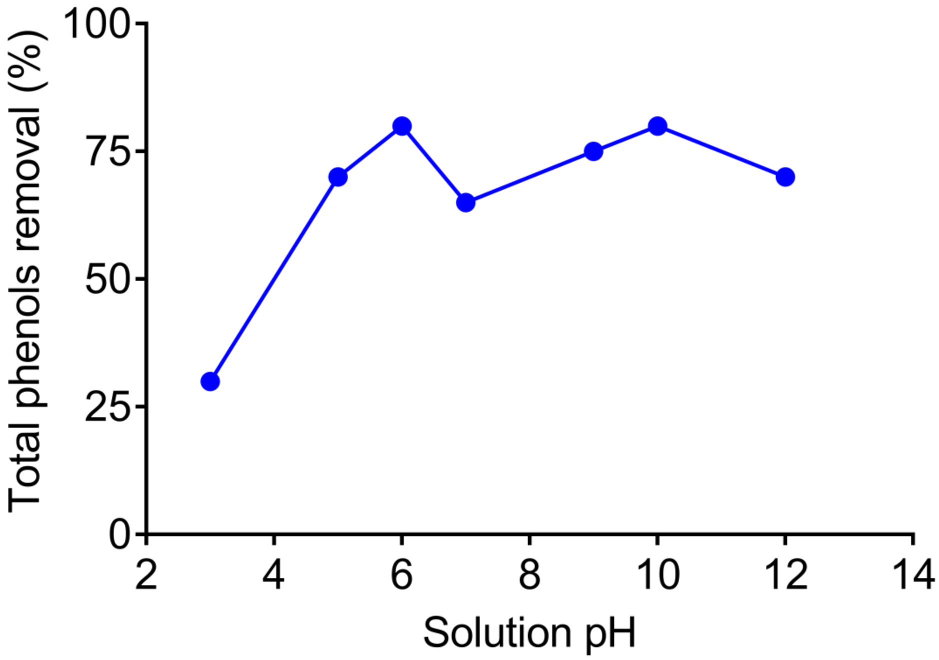

Figure 9: Influence of OWW pH on BCO–NC removal efficiency

Specifically, two different interactions might have occurred simultaneously as follows (i) electron exchange between the basic surface groups of the BCO–NC and the aromatic rings (ii) electrostatic interactions when the solution pH is higher or lower than the pH_{pzc} of the BCO–NC. At pH 3, 29% of total phenols were removed, and it increased to 82% when the pH increased to 6 then decreased at pH 7. A sudden rise in the removal efficiency was seen beyond pH 7. Hence, it is concluded that the BCO–NC is efficient to remove polyphenols from the OWW.

3.2.4 Influence of Feed Concentration

The influence of the feed concentration on the total phenol removal by BCO–NC was investigated at pH 6 using 1.0 g BCO–NC by varying the initial total phenols concentration (50–500 mg/L). The total phenols removal efficiency increases steadily as the initial concentration increases as seen in Figure 10. About 17% total phenols were removed when the concentration was 50 mg/L, and it increased beyond 80% at 500 mg/L. The increasing trend could be as a result of driving force provided by the higher initial phenol concentration to overcome the mass transfer flux of the variety of polyphenols in the presence of BOC–NC (Ngwabebhoh et al., 2016).

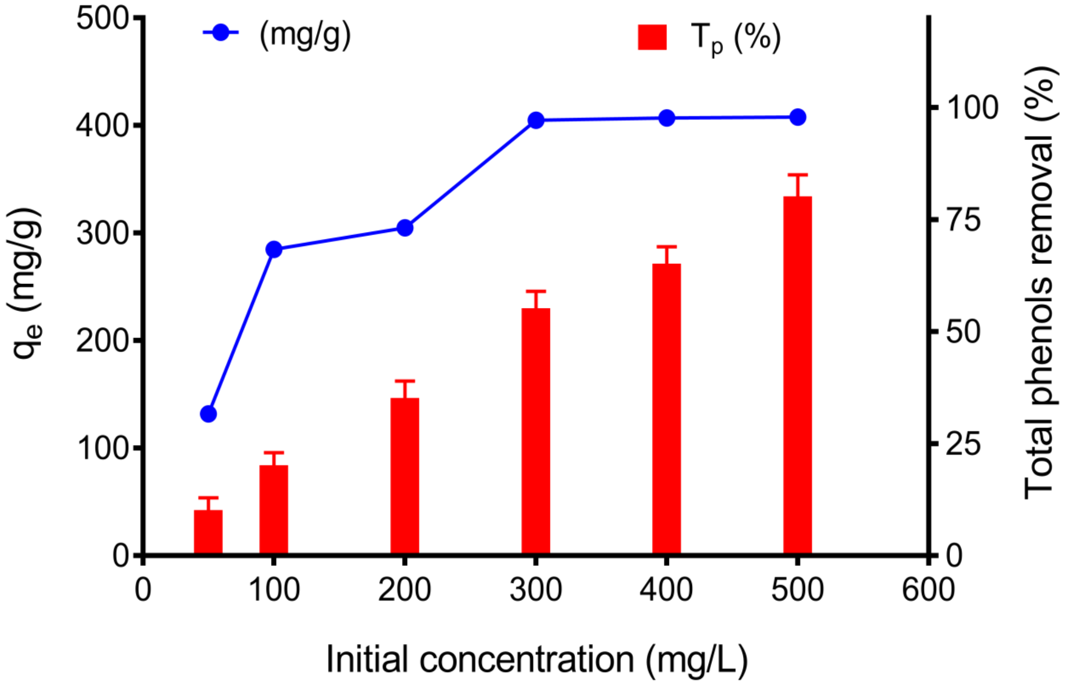

Figure 10: Effect of feed concentration on BCO–NC removal efficiency

However, it is observed that the BCO–NC exhibited different uptake patterns. The uptake capacity increased from 130 mg/g at 50 mg/L in a step-wise manner until equilibrium was attained at 300 mg/L where about 400 mg/g total phenols had been adsorbed by BCO–NC. Meanwhile, the BCO–NC removal efficiency extends beyond 300 mg/L. Thus, BCO–NC can be employed for the treatment of both dilute and highly concentrated polyphenols-laden industrial effluents.

3.3 Photo-reductive Experiments

Even though the olive cake has no photoactivity character, the CuO nanoparticles integrated on its surface possesses excellent photo-reductive activity. Tamuly et al. (2014) reported that bio-derived CuO nanoparticles exhibited comparative photocatalytic when applied to degrade methyl red dye in the presence of commercial CuO nanoparticles.

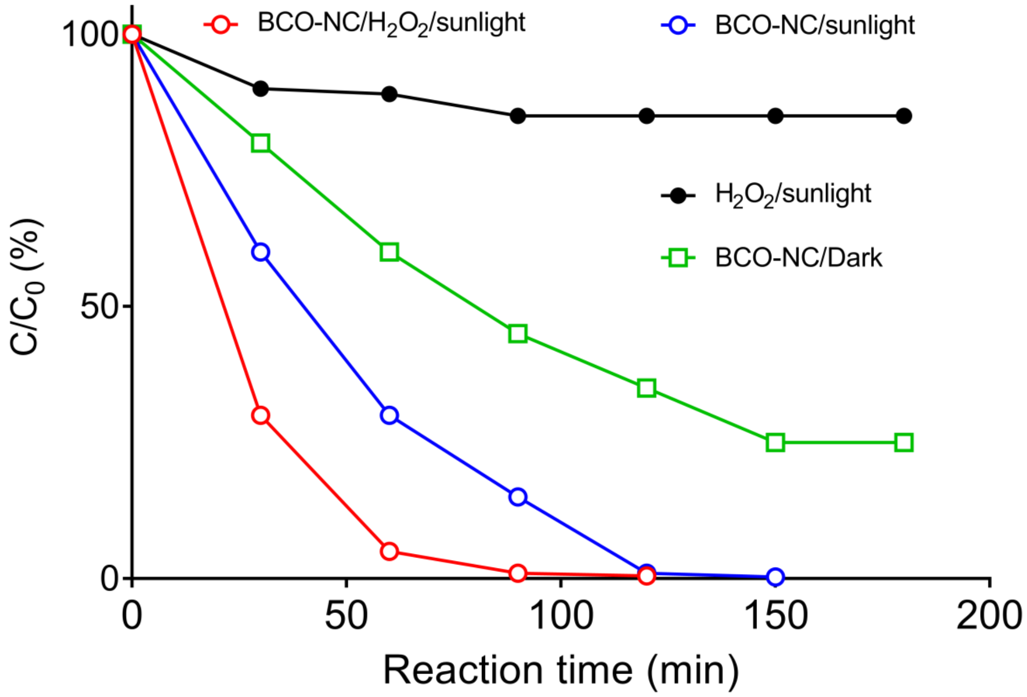

Figure 11: Sunlight assisted removal of total phenols from OWW (H2O2; 1 mM, pH; 10 and BCO–NC; 1.0g, initial phenol concentration; 800 mg/L)

Here, various experiments were performed to investigate the photosensitive activity of the BCO–NC. As shown in Figure 11, only 20% total phenols were removed after 180 min when H_2O_2/sunlight was applied in the absence of BCO–NC. This could be as a result of insufficient generated hydroxyl radicals required to degrade the varieties of phenolic compounds in the OWW. About 76% total phenol was removed after 180 min in the absence of sunlight (dark) when BCO–NC was utilised at pH 10.

The total phenols removal rate increased in BCO–NC/sunlight system from 40% to 80% as the reaction progressed from 30 min to 90 min.

Interestingly, complete phenol removal was noticed at about 130 min of the experiment. This suggests that the CuO in the BCO–NC enhanced the polyphenol removal via photocatalytic reduction of the phenolic compounds and subsequent adsorption by the olive cake in the backbone of the nanocomposite. Thus, a synergistic behaviour contributed to the rapid and enhanced removal of total phenols from the OWW. In the BCO–NC/H2O2/sunlight, the removal rate increased rapidly, and a complete removal was observed at about 90 min of the experiments. Hence, it is concluded that the BCO–NC aided the generation of more hydroxyl radicals from the H_2O_2 and thus resulted in enhanced removal rate.

3.3.1 Effect of BCO–NC Dosage under Sunlight

The influence of BCO–NC doses under sunlight in the absence of hydrogen peroxide was considered. As shown in Figure 12, after 30 min of solar irradiation 25, 29 and 43% total phenols were removed when 1.5, 0.5 and 1.0 g BCO–NC were introduced into the reaction system, respectively. As the reaction progressed, the removal efficiency increased, and a complete removal of polyphenol was achieved at 120, 150 and 180 min for 1.0, 0.5 and 1.5g of BCO–NC respectively. Hence, 1.0g is applied for the rest of the experiments, and this confirms that sizeable quantity of the fabricated nanocomposite is required to achieve total removal of phenolic compounds from organic-bearing oily wastewater (Nguyen et al., 2015).

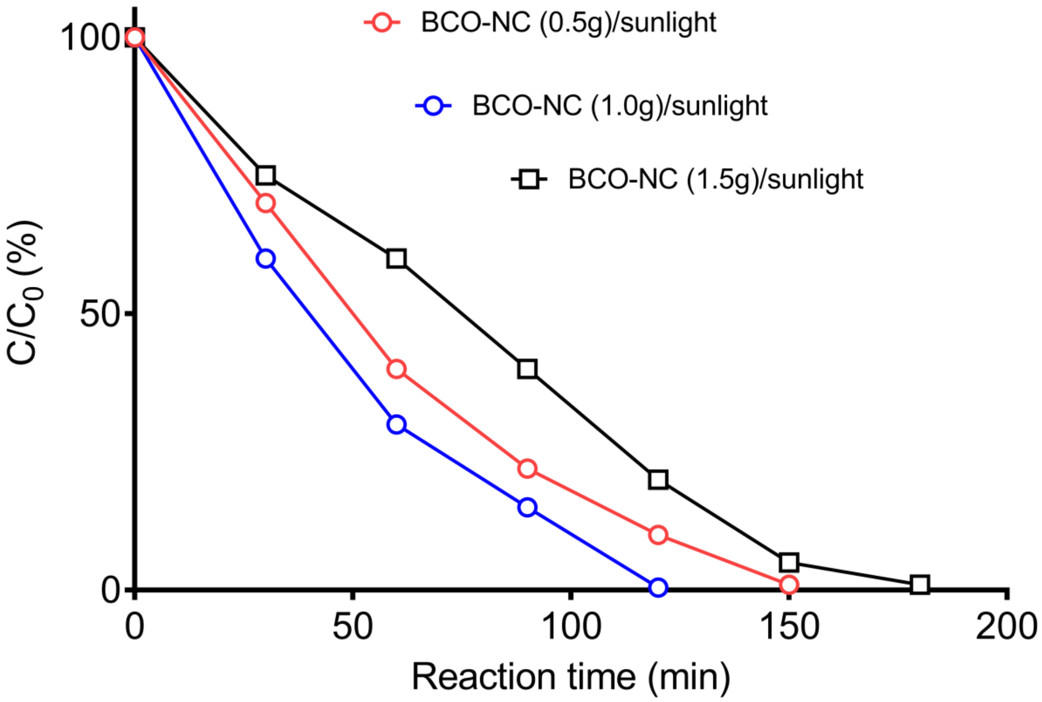

Figure 12: Influence of BCO–NC doses under sunlight in the absence of H2O2 (pH; 10 and initial phenol concentration; 800 mg/L)

3.3.2 Effect of pH Under Sunlight

The impact of varying the pH of the OWW under solar irradiation for the removal of total phenols was investigated (initial phenol concentration 800 mg/L, 1.0 g BCO–NC and 180 min solar irradiation). The highest total phenol removal rate was obtained at pH 10 after 180 min. At the end of the experiment as shown in Figure 13, pH 3.0 gave the lowest polyphenol removal (70%), it is important to stress that this three times the amount of polyphenols removed in the dark at same pH. The removal rate of total phenol in the absence of H_2O_2 at pH 10 decreased and extended to 180 min which is twice (90 min) of what was reported in the presence of H_2O_2 (section 3.3). This decrease in removal rate is likely due to lack of hydroxyl radicals that enhances the photoactivity of the BCO–NC (Alalm et al., 2014).

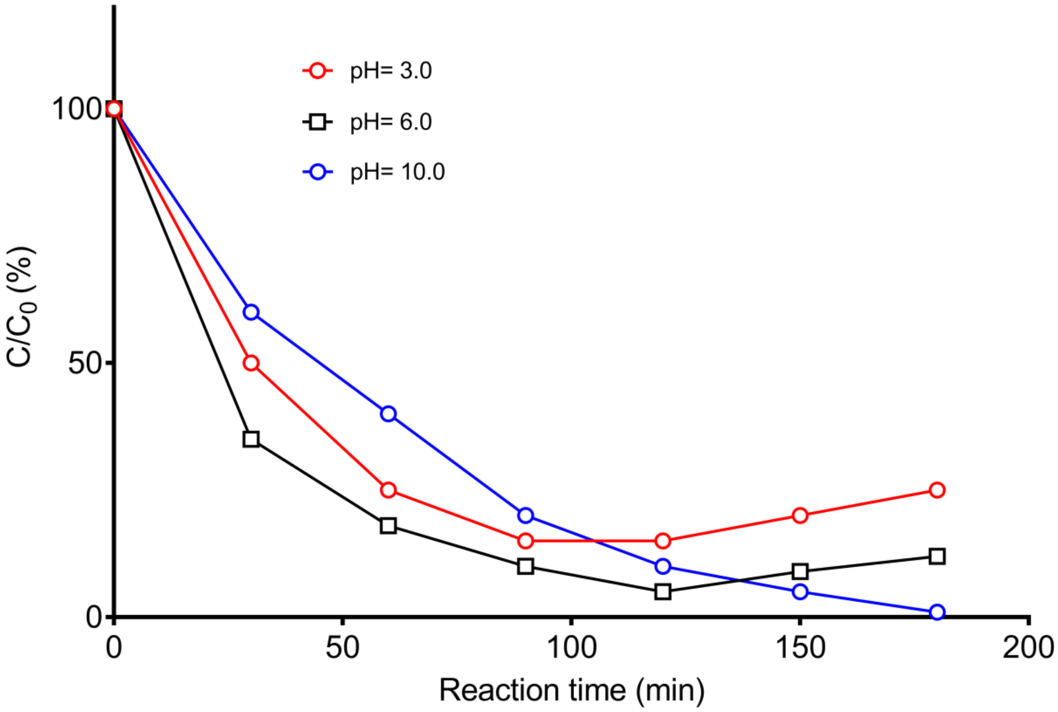

Figure 13: Effect of solution pH in the absence of H_2O_2

3.3.3 Effect of Hydrogen Peroxide on Total Phenol Removal

According to previous studies, the H_2O_2 efficiently enhanced the photo-reduction of bio-calcitrant in organic-laden wastewaters. Specifically, the hydrogen peroxide oxidises the polyphenols in the OWW directly to less harmful products (CO_2 and H_2O), thus, reducing the toxicity of the olive mill wastewater. Figure 14 represents the effects of various concentrations of hydrogen peroxide on the removal of polyphenols contained in the OWW. The reaction was performed at pH 10 under sunlight in the presence of 1.0 g of BCO–NC.

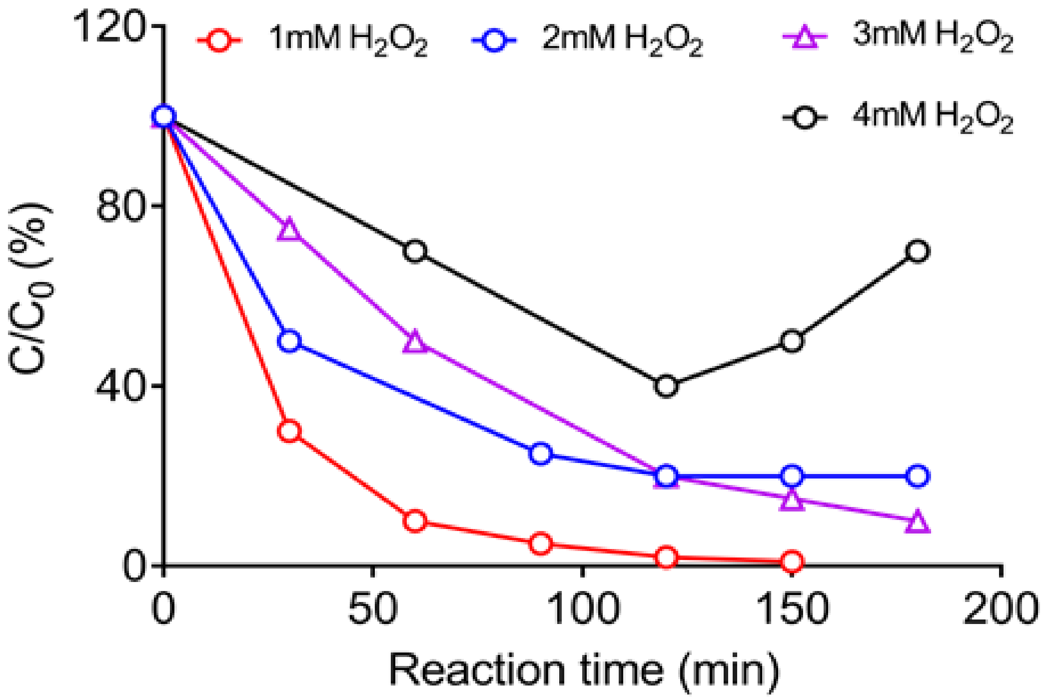

Figure 14: Effect of hydrogen peroxide concentration on total phenol removal

As seen, the photo-reduction of the total phenol was observed to be slow in the presence of high concentrations of hydrogen peroxide. This observation is probably due to excessive generation of hydroxyl radicals in the reaction system, hence, inhibiting the polyphenol removal. About 60% total phenol was removed in 120 min when 4 mM of H_2O_2 was introduced into the reaction system, but beyond 120 min, the removal efficiency decreased significantly to 25%.

Similarly, 86 and 90% total phenol was removed after 180 min when 2.0 mM and 3.0 mM H_2O_2 was introduced to the reaction system. Contrastingly, a complete removal of total phenol was observed in the presence of BCO-NC/1mM H2O2/sunlight in less than 150 min. This rapid removal is likely due to the generation of the quantitative amount of hydroxyl radicals required to initial the degradation of the aromatic rings of the polyphenols (Xu and Wang, 2011). Therefore higher amounts of hydrogen peroxide are not recommended for the removal of the total phenol from the OWW. A similar trend has been reported by Oladipo et al. 2016 using magnetic composite for degradation of antibiotics and phenol.

3.4 Sorption Kinetics

The adsorption rate mechanism was examined by fitting the experimental data of both the laboratory and sunlight assisted phenol reduction to the Elovich, pseudo-first order, fractional power, pseudo-second-order, Avrami and intraparticle diffusion models. The parameters of each kinetic model are obtained using the following equations respectively:

$$q_t = \frac{1}{\beta}\ln(\alpha\beta t) \tag{7}$$

$$q_t = q_e\left(1 - e^{-k_1 t}\right) \tag{8}$$

$$q_t = k_f t \tag{9}$$

$$\frac{t}{q_t} = \frac{1}{k_2 q_e^2} + \frac{t}{q_e} \tag{10}$$

$$q_t = q_e\left(1 - e^{-\left[(k_{Av} t)^{nAV}\right]}\right) \tag{11}$$

$$q_t = k_i t^{0.5} + C \tag{12}$$

Where q_e and q_t represent the quantity of total phenol removed per BCO–NC mass unit (mg/g) at equilibrium and time t, respectively. The rate constants are k_1 (1/min), k_i (mg/g min$^{0.5}$), k_2 (g/mg min), k_{Av} (1/min) and k_f (mg/gmin^{-v}) for the pseudo-first order, intraparticle diffusion, pseudo-second order, Avrami and fractional power models, respectively. The desorption constant and initial adsorption rate for the Elovich model are represented by α and β, respectively (Hossain et al., 2012; Pellera and Gidarakos, 2015).

After fitting the experimental data to the afore-mentioned kinetic models, the parameters obtained are displayed in Table 7. Based on the R^2 and RSS values, the experimental results could not be described by pseudo-first order, Elovich and Avrami models (Gupta and Babu, 2009; Pellera and Gidarakos, 2015). However, intraparticle diffusion provides a better description with its lowest RSS values. It is important to stress that the data appear to be suitably fitted to the pseudo-second order kinetics.

Therefore, the mechanism of total phenol removal involves electron sharing or exchange (chemisorption) between the aromatic rings of the polyphenols and basic functional groups of the BCO–NC. Also, rapid intraparticle diffusion of the phenolics to the pores of the BCO–NC may also contribute to the phenol removal (Ho, 2006). The fitness of each kinetic model in the dark and sunlight assisted treatment is ranked based on the RSS, and R^2 values and the graphical illustration of the ranking order is shown in Figure 15.

Table 7: Kinetic details for total phenol removal using BCO-NC

Kinetic models	**Parameters**	**Dark**	**Sunlight**
Pseudo-first order	q_e	334.8	589.9
	k_1	0.0134	0.0117
	R^2	0.878	0.723
	RSS	3.8921	4.8912
Elovich	α	1.57.E + 34	1.04.E + 18
	β	0.9874	0.7766
	R^2	0.921	0.956
	RSS	1.9811	3.9871
Pseudo-second order	q_e	645.9	792.8
	k_2	0.0068	0.0019
	R^2	**0.998**	**1.000**
	RSS	**0.5466**	**0.6991**
Avrami	q_e	456.9	689.5
	k_{Av}	4.5244	4.8855
	R^2	0.679	0.567
	RSS	8.1191	6.9812
Intraparticle diffusion	k_i	0.1161	0.1213
	C	30.89	28.09
	R^2	**0.994**	**0.997**
	RSS	**0.2471**	**0.2119**
Fractional power	k_f	29.071	26.089
	v	0.0276	0.0314
	R^2	0.967	0.988
	RSS	2.0811	1.4511
Experimental	$q_{e,exp}$ (mg/g)	665.9	802.6

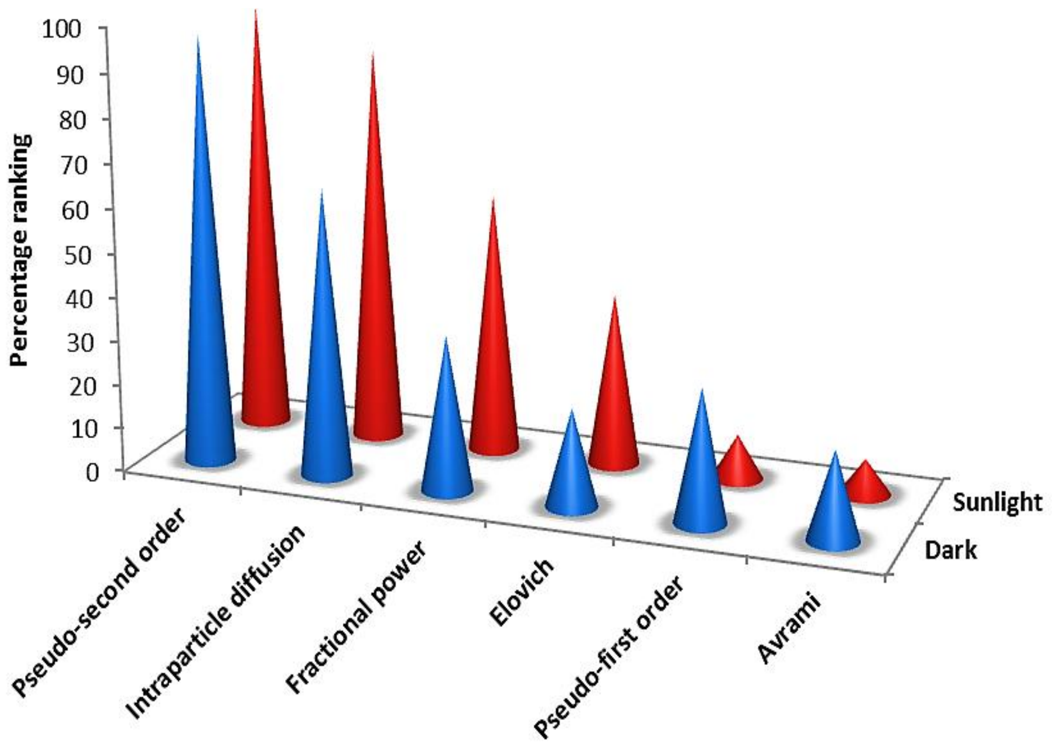

Figure 15: Ranking of kinetic models in sunlight and dark experiments

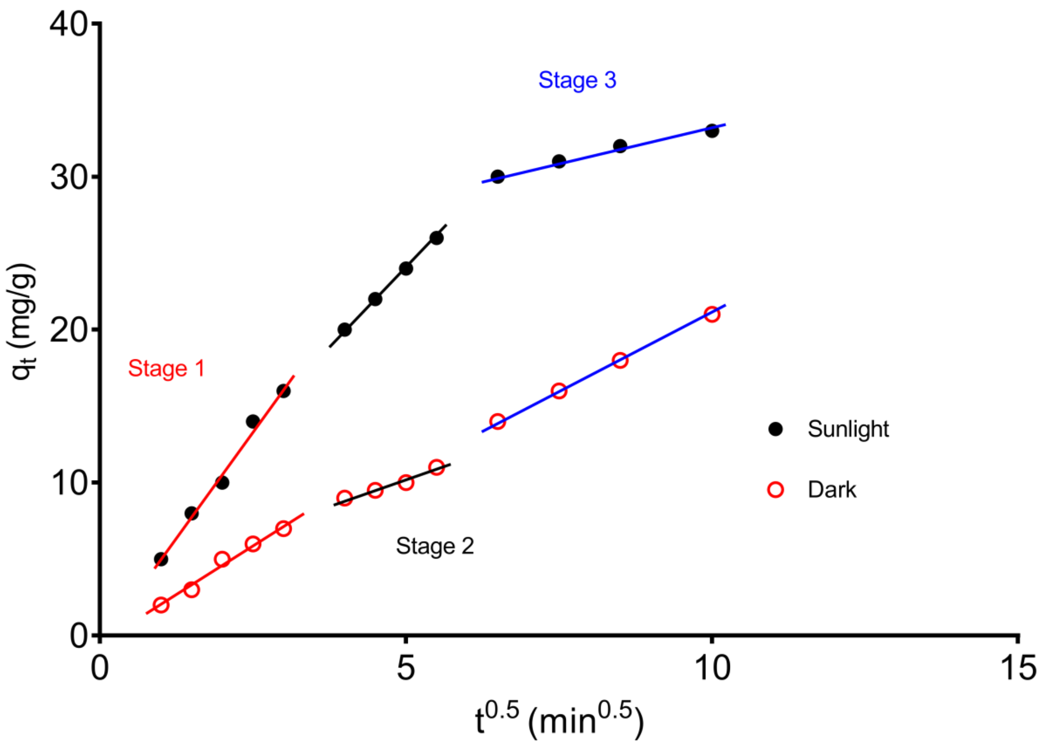

Figure 16: Intraparticle diffusion of polyphenols into BCO-NC adsorbent

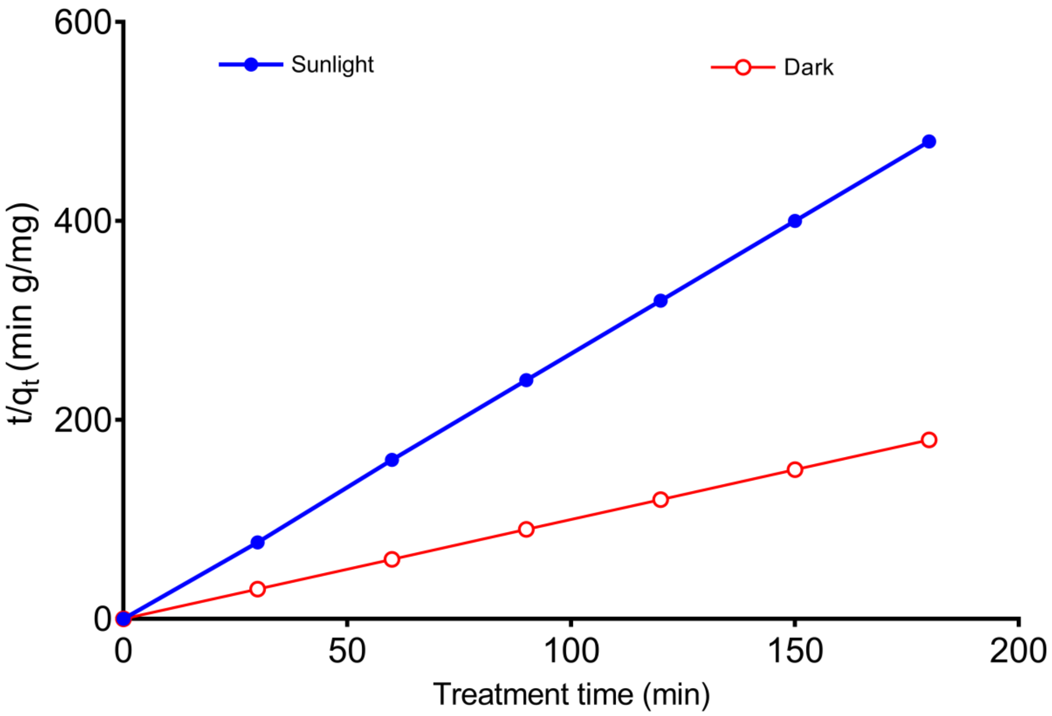

Figure 17: Pseudo-second order sorption rate mechanism for BCO-NC

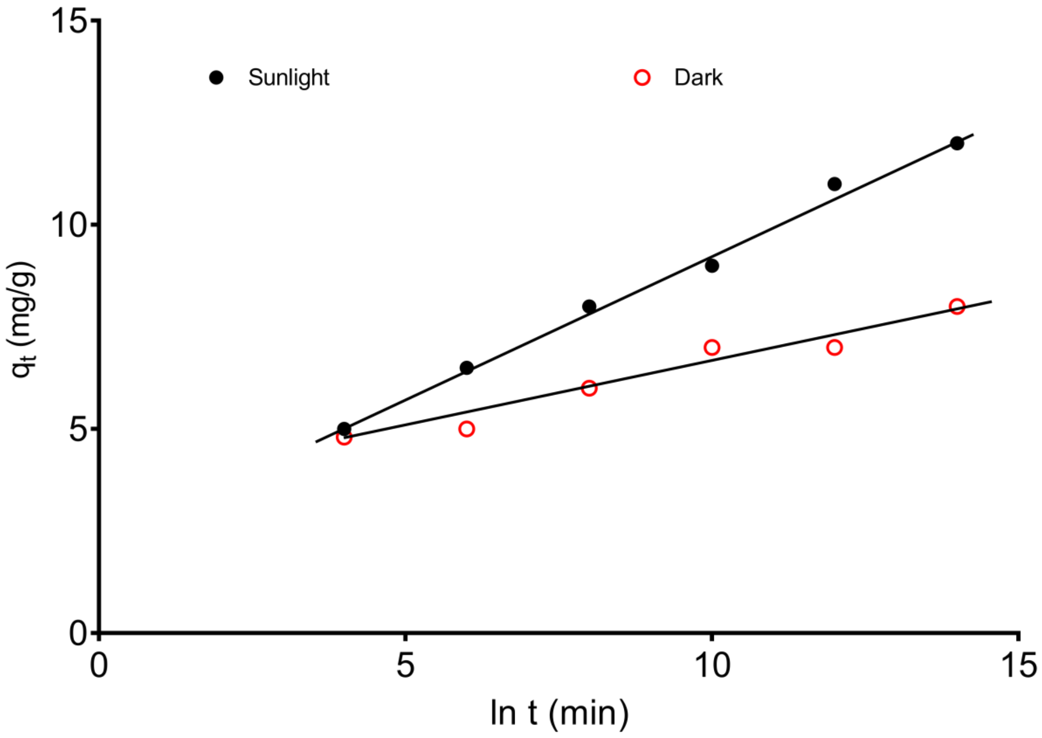

Figure 18: Elovich sorption rate for polyphenol by BCO-NC

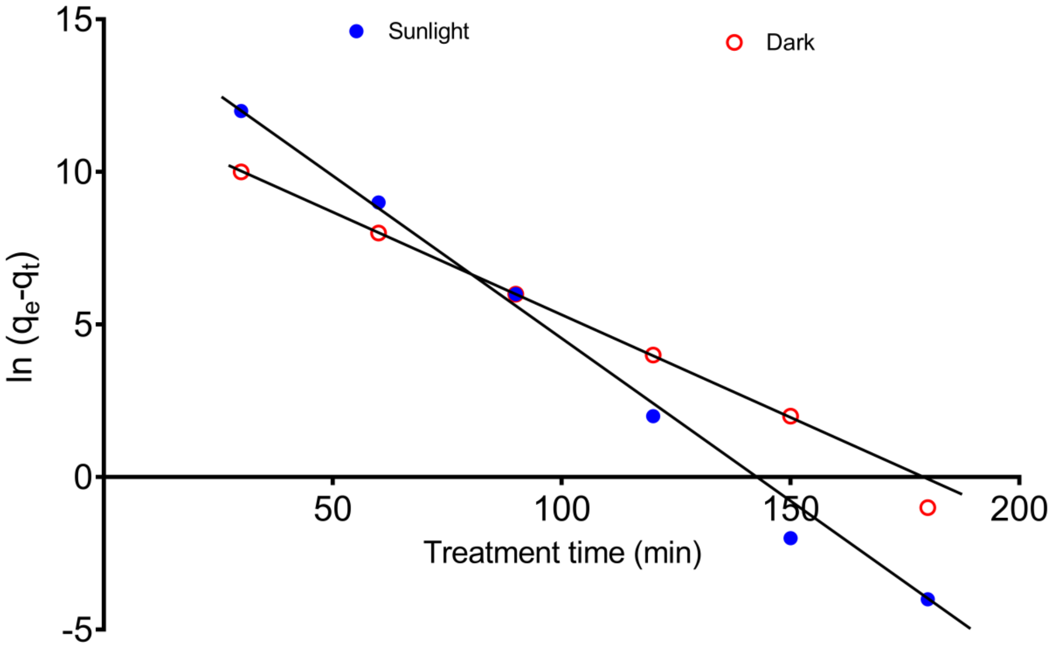

Figure 19: Pseudo-first order sorption kinetics for BCO-NC

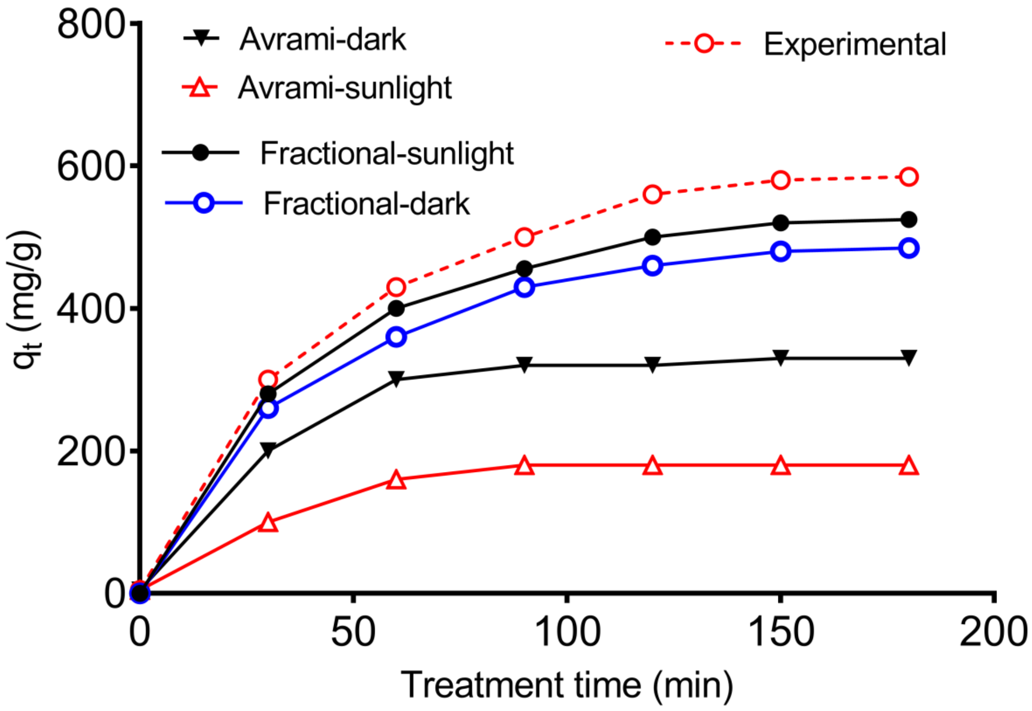

Figure 20: Avrami and fractional power kinetic models for polyphenol removal

3.5 Adsorption Isotherm

The adsorption mechanism of the BCO-NC can be followed by fitting the experimental data into isotherm models. The equilibrium parameters obtained from the isotherm model describe the reaction pathway of the adsorbate in the presence of the adsorbent and provide detailed information regarding the kind of interaction in the reaction medium (Fayazi et al., 2015). Here, the experimental results were fitted into the two commonly used isotherm models (Langmuir and Freundlich) and the parameters are obtained according to the following equations, respectively (Song et al., 2016):

$$\frac{C_e}{q_e} = \frac{1}{q_m K_L} + \frac{C_e}{q_m} \tag{13}$$

$$\ln q_e = \ln k_f + \frac{1}{n} \ln C_e \tag{14}$$

Where C_e (mg/L) and q_e (mg/g) are the equilibrium total phenol concentration and amount of total phenol removed at equilibrium time, respectively. The q_m (mg/g) represent the maximum amount of total phenol removed. The Langmuir and Freundlich constants are denoted by K_L (L/mg) and n respectively.

The Langmuir model is based on the assumption that monolayer reactions take place at the interphase of the adsorbent and the adsorbate using uniform energy levels. The isotherm equally assumes the lack of interactions or transmigration of the adsorbed molecules on the adsorbent surface. Contrastingly, the Freundlich model describes multilayer (heterogeneous) interactions between the adsorbate and the adsorption sites occurring at different energy levels (Fayazi et al., 2015; Oladipo and Gazi, 2014).

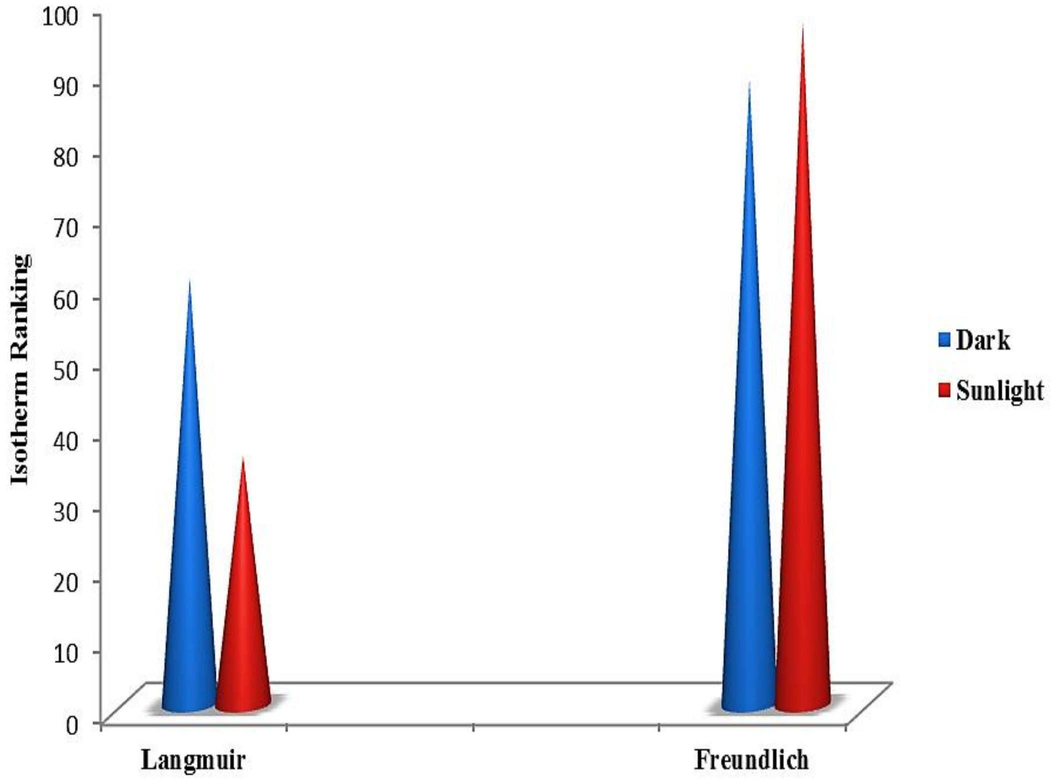

Figure 21: Ranking of the most suitable isotherms for polyphenol removal from OWW

The respective parameters obtained from Langmuir and Freundlich isotherms are presented in Table 8. According to the values of R^2 and RSS, the total phenol removal by BCO-NC was well fitted to the Freundlich model. The lower the RSS values, the more suitable is the model, on the other hand, R^2 values near unity are voted to fit the experimental date well. As a result of the Freundlich fitness, it is concluded that the removal mechanisms occur at heterogeneous adsorption sites on BCO-NC, hence, forming multilayer coverage of polyphenols on the entire surface of the BCO-NC.

Table 8: Isotherm details for total phenol removal using BCO-NC

Condition	**Model**	**BCO-NC dosage (g)**			**Solution pH**		
		0.5	1.0	2.5	3	6	10
Sunlight	***Langmuir***						
	q_m (mg/g)	437.5	696.5	657.7	355.9	509.4	689.3
	K_L (L/mg)	0.56	0.11	3.15	1.78	3.12	5.88
	R^2	0.987	0.979	0.789	1.000	0.923	0.939
	RSS	7.1812	5.819	3.123	0.3121	1.345	5.126
	Freundlich	134.8	345.8	569.5	321.5	432.9	549.8
	K_F (mg/g)	63.8	45.6	28.3	76.3	33.9	23.9
	n	1.99	1.89	3.46	5.25	2.51	3.77
	R^2	0.996	0.998	0.998	0.999	0.997	0.999
	RSS	0.1231	0.1441	0.1631	0.1211	0.2081	0.3213
Dark	***Langmuir***	325.9	413.9	697.6	329.5	541.8	478.9
	q_m (mg/g)	549	378	209	298	388	511
	K_L (L/mg)	3.65	2.56	1.99	4.88	3.98	2.67
	R^2	0.899	0.786	0.911	0.931	0.934	0.978
	RSS	3.891	4.981	3.234	11.13	9.121	7.123
	Freundlich	244.9	321.8	534.9	309.3	334.6	534.6
	K_F (mg/g)	71.3	34.3	11.8	89.3	53.7	9.81
	n	1.49	2.44	3.33	5.33	5.26	6.45
	R^2	0.996	0.991	1.000	0.998	1.000	0.997
	RSS	0.2981	0.3211	0.3412	1.4511	0.9121	0.6712

The values of the *n* constant of the Freundlich isotherm are also greater than 1, confirming a favourable process (Song et al., 2016). It is important to stress that the maximum quantity of polyphenol removed is approximately 696.5 mg/g in the sunlight which could be as a result of the presence of hydrogen peroxide that aided the photo-reductive potential of the CuO on the surface of the olive cake powder. About 413.9 mg/g total phenol was removed in the dark experiment under the same pH and BCO–dosage like those of sunlight experiment. Since polyphenol is majorly responsible for the OWW colour, hence, the higher the total phenol removed, the less coloured the OWW solution as shown in Figure 22.

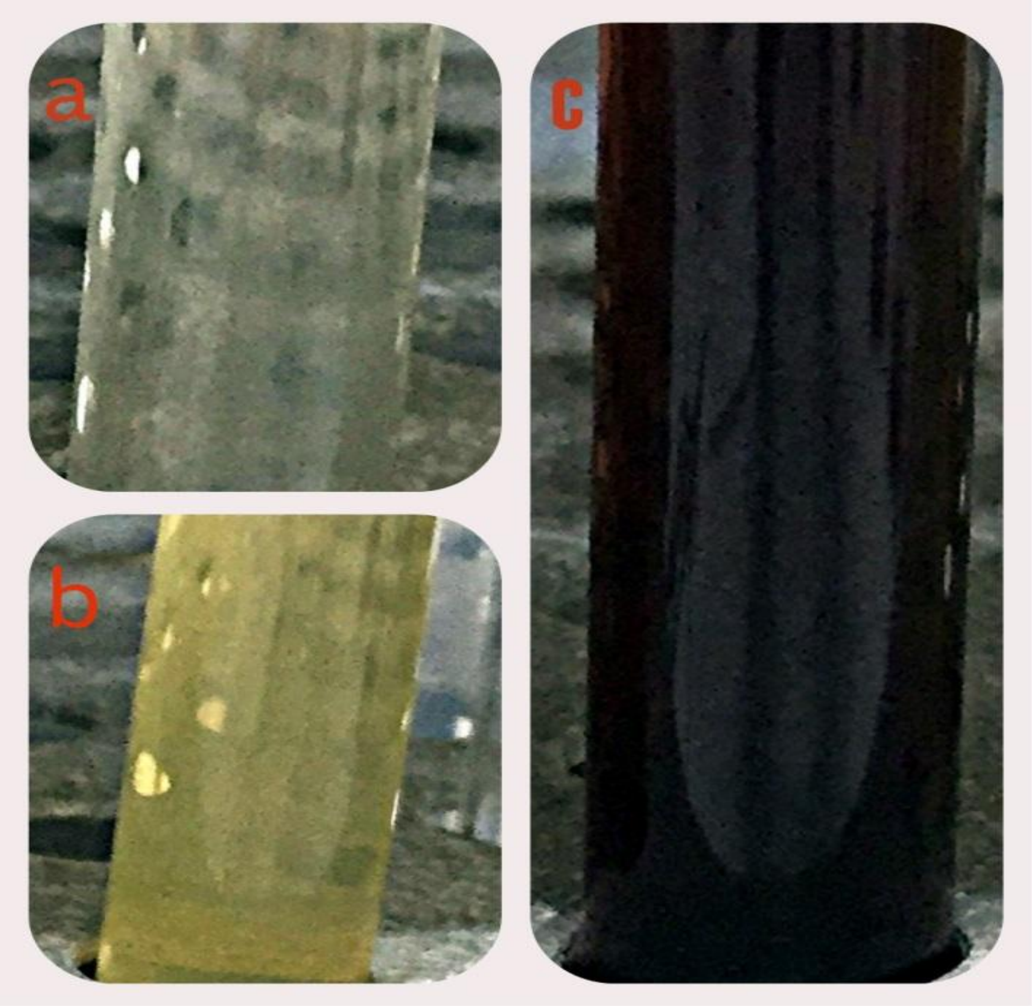

Figure 22: Coloration variation as a function of polyphenol removal (a) Sunlight assisted treatment (b) dark treatment using BCO-NC (c) untreated olive mill wastewater

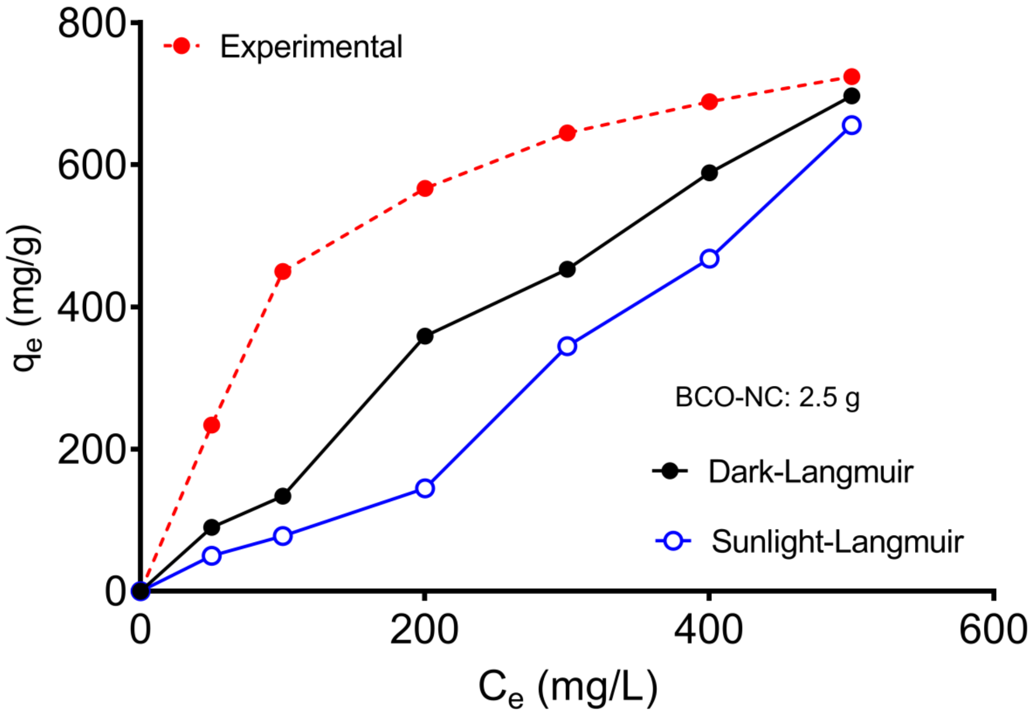

Figure 23: Langmuir isotherm of total phenols removal by BCO–NC

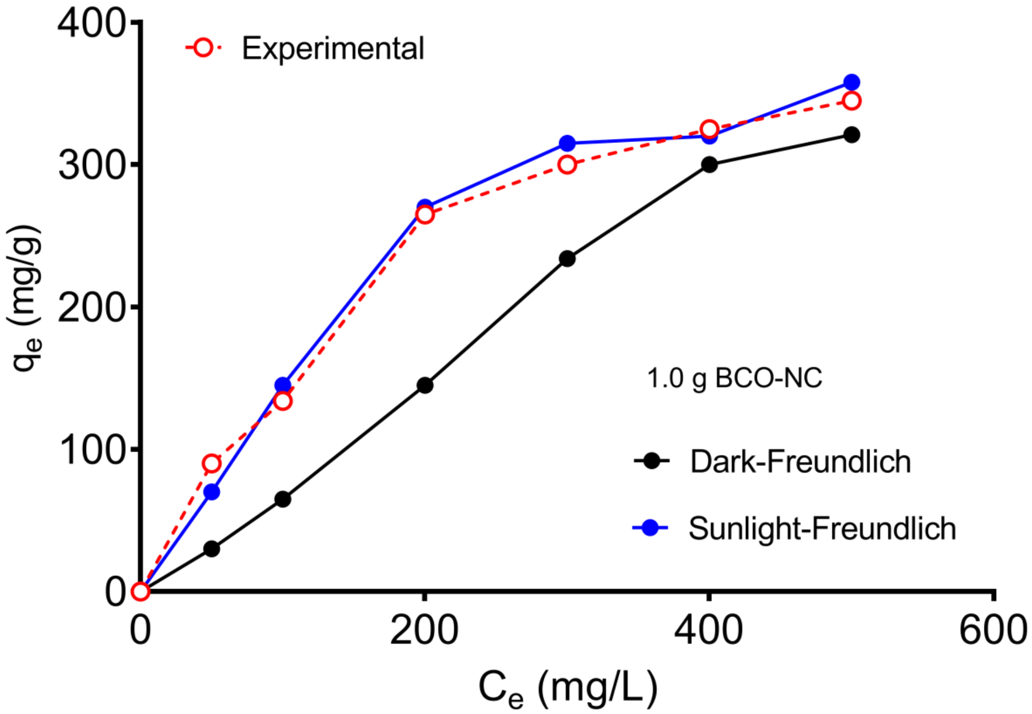

Figure 24: Freundlich isotherm for the removal of total phenols by BCO–NC

3.6 Recommendation for OWW Management in Cyprus

According to the experimental results and observations from the current research, some recommendations have been highlighted to reinforce feasibly and sustainable management of olive mill wastes in Cyprus:

- Spatial survey and quantitative assessment of olive processing mills located in Northern Cyprus must be a top priority for the scholars.
- Periodical monitoring of OWW discharge from identified olive mill processor must be implemented as part the olive mill waste management policy
- Awareness must be raised among olive oil processor concerning the environmental impact of improper disposal of OWW to the environment.
- Storage and conversion of solid olive wastes to an efficient adsorbent under optimised conditions must be given priority.
- Fabrication of low-cost treatment plant for pretreatment and reuse of olive mill wastewater is recommended.

The recommendations presented here call for further research to optimise the total phenol removal strategy using bio-derived olive mill-based wastes and investigate the presence of interfering metal ions in the reaction system. The effects of synergistic and competitive adsorption of inorganic compounds in OWW on total phenol removal should be checked in the next research. Deep insight into the modification of olive mill solid wastes to enhance its affinity toward total phenol removal from OWW must be given priority. The potential and performance of olive mill solid wastes in simulated fixed-bed adsorption must be investigated for phenol removal.

Chapter 4

CONCLUSION

The total phenol of olive mill wastewater was successfully reduced using CuO/olive cake nanocomposite, and the conclusions were reached:

- High-performance nanocomposite was obtained via an environmentally benign strategy without the use of expensive and toxic chemicals.
- The fabricated CuO/olive cake nanocomposite efficiently outperformed most reported adsorbents for total phenol removal from olive mill wastewater.
- It is observed that the total phenol removal is dependent on the BCO–NC concentration, hydrogen peroxide doses and the feed concentration.
- About 80% total phenols were removed after 180 min in the dark using BCO–NC. However, the total phenol removal increased to 100% within the first 90 min when BCO-NC/H_2O_2/sunlight system was used.
- The R^2 and RSS values confirmed that the experimental results could not be described by pseudo-first order, Elovich and Avrami models. On the other hand, the experimental data appear to be suitably described by the intraparticle diffusion and pseudo-second order kinetics.
- The sorption mechanism was suitably described by Freundlich isotherm, thus indicating a multilayer interaction between the BCO–NC and the phenolic compounds in the OWW.

REFERENCES

Achak, M., Hafidi, A., Ouazzani, N., Sayadi, S., & Mandi, L. (2009). Low cost biosorbent "banana peel" for the removal of phenolic compounds from olive mill wastewater: Kinetic and equilibrium studies. *J. Hazard. Mater*. 166, 117–125.

Aladham, R. A. F. (2012). Removal of Polyphenols from Olive Mill Wastewater using Activated Olive Stones. Master thesis submitted An-Najah National University, Palestine.

Anastasiou, C. C., Christou, P. Michael, A. Nicolaides, D. & Lambrou, T. P. (2011) Approaches to olive mill wastewater treatment and disposal in Cyprus. *J. Environ. Res*. 5, 49–58.

Azbar, N., Bayram, A., Filibeli, A., Muezzinoglu, A., Sengul, F., & Ozer, A. (2004). A review of waste management options in olive oil production. *Critical Rev. Environ. Sci. Technol.* 34, 209–247.

Cox, L., Celis, R., Hermosin, M. C., Becker, A. & Cornejo, J. (1997). Porosity and herbicides leaching in soils amended with olive mill wastewater. *J. Agric. Ecosyst. Environ*. 65, 151–162.

Daâssi, D., Lozano-Sánchez, J. Borrás-Linares, I., Belbahri, L., Woodward, S., Zouari-Mechichi, H., Mechichi, T., Nasri, M., Segura-Carretero, A. (2014).

Olive oil mill wastewaters: Phenolic content characterization during degradation by *Coriolopsis gallica*. *Chemosphere*, 113, 62–70.

Fayazi, M., Ghanei-Motlagh, M., & Taher, M. A. (2015). The adsorption of basic dye (Alizarin red S) from aqueous solution onto activated carbon/γ-Fe_2O_3 nano-composite: kinetic and equilibrium studies. *Mater. Sci. Semicond. Process*. 40, 35–43.

Frankel, E., Bakhouche, A. Lozano-Sánchez, J., Segura-Carretero, A., Fernández-Gutiérrez, A. (2013). Literature review on production process to obtain extra virgin olive oil enriched in bioactive compounds. Potential use of byproducts as alternative sources of polyphenols. *J. Agric. Food Chem*. 61, 5179–5188.

Greenberg, A. E., Clesceri, L. S., & Eaton, A. D. (1992). Standard methods for the examination of water and wastewater. APHA/AWWA/WEF, 16th Ed., Washington, DC, Cabs.

Hazarika, M., Saikia, I., Das, J., Tamuly, C., & Das, M. R. (2016). Biosynthesis of $Fe_2O_3@SiO_2$ nanoparticles and its photocatalytic activity. *Mater. Lett*. 164, 480–483.

Ho, Y. S. (2006). Review of second-order models for adsorption systems. *J. Hazard. Mater*. 136, 681–689.

Hossain, M. A., Ngo, H. H., Guo, W. S., Nguyen, T. V. (2012). Palm oil fruit shells as biosorbent for copper removal from water and wastewater: experiments and sorption models. *Bioresour. Technol*. 113, 97–101.

Kalogerakis, N., Politi, M., Foteinis, S., Chatzisymeon, E., & Mantzavinos, D. (2013). Recovery of antioxidants from olive mill wastewaters: A viable solution that promotes their overall sustainable management. *J. Environ. Manage*. 128, 749–758.

Khan, M. A., Ngabura, M., Choong, T. S. Y. Masood, H., & Chuah, L. A. (2012). Biosorption and desorption of Nickel on oil cake: Batch and column studies. *Biores. Technol*. 103, 35–42.

Komnitsas, K., & Zaharaki, D. (2012). Pre-treatment of olive mill wastewaters at laboratory and mill scale and subsequent use in agriculture. Legislative framework and proposed soil quality indicators. *Res. Cons. Recycl.* 69, 82–89.

Nassar, N. N., Arar, L. A. Marei, N. N., Abu Ghanimb, M. M., Dwekat, M. S., & Sawalha, S. H. (2014). Treatment of olive mill based wastewater by means of magnetic nanoparticles: Decolourization, dephenolization and COD removal. *Environ. Nanotechnol. Monit. Manage*. 1–2, 14–23.

Nguyen, T. A. H., Ngo, H. H., Guo, W. S., Pham, T. Q., Li, F. M., Nguyen, T. V., & Bui, X. T. (2015). Adsorption of phosphate from aqueous solutions and sewage using zirconium loaded okara (ZLO): Fixed-bed column study. *Sci. Total Environ*. 523, 40–49.

Ngwabebhoh, F. A., Gazi, M. & Oladipo, A. A. (2016). Adsorptive removal of multi-azo dye from aqueous phase using a semi-IPN superabsorbent chitosan-starch hydrogel. *Chem. Eng. Res. Des*. doi:10.1016/j.cherd.2016.06.023.

Niaounkais, M. & Halvadakis, C. P. (2004). Olive–Mill Waste Management: Literature Review and Patent Survey. 1st edition, Athens, *Typothito George Dardanos*, 407.

Nogueira, V., Lopes, I., Freitas, A. C., Rocha-Santos, T. A. P., Gonçalves, F., Duarte, A. C., & Pereira, R. (2015). Biological treatment with fungi of olive mill wastewater pre-treated by photocatalytic oxidation with nanomaterials. *Ecotoxicol. Environ. Saf.* 115, 234–242.

Ntougias, S., Bourtzis, K., & Tsiamis, G. (2013). The microbiology of olive mill wastes. *BioMed Res. Int*. http://dx.doi.org/10.1155/2013/784591.

Obied, H. K. Bedgood Jr., D. R. Prenzler, P. D. & Robards, K. (2007). Bioscreening of Australian olive mill waste extracts: biophenol content, antioxidant, antimicrobial and molluscicidal activities. *Food Chem. Toxicol*. 45, 1238–1248.

Oladipo, A. A., & Gazi, M. (2014). Nickel removal from aqueous solutions by alginate-based composite beads: Central composite design and artificial neural network modeling. *J. Water Process Eng*. 8, e81–e91.

Oladipo, A. A., & Gazi, M. (2015). Microwaves initiated synthesis of activated carbon-based composite hydrogel for simultaneous removal of copper (II) ions and direct red 80 dye: A multi-component adsorption system. *J. Taiwan Inst. Chem. Eng*. 47, 125–136.

Oladipo, A. A., Gazi, M., & Elvan, Y. (2015). Single and binary adsorption of azo and anthraquinone dyes by chitosan-based hydrogel: Selectivity factor and Box-Behnken process design. *Chem. Eng. Res. Des*. 104, 264–279.

Oladipo, A. A., Abureesh, M. A., & Gazi, M. (2016). Bifunctional composite from spent "Cyprus coffee" for tetracycline removal and phenol degradation: Solar-Fenton process and artificial neural network. *Int. J. Biol. Macromol*. 90, 89–99.

Ouzounidou, G., Asfi, M., Satirakis, N., Papadopoulou, P., & Gaitis F. (2001). Olive mill wastewater triggered changes in physiology and nutritional quality of tomato. *J. Terrest. Aqua. Environ. Toxicol.-Global Sci. Books*, 1, 1–30.

Ozkaya, B. (2006). Adsorption and desorption of phenol on activated carbon and a comparison of isotherm models. *J. Hazard. Mater*. B 129, 158–163.

Paraskeva, C. A., Papadakis, V. G., Kanellopoulou, D. G., Koutsoukos P. G., & Angelopoulos, K. C. (2007). Membrane filtration of olive mill wastewater (OMW) and OMW fractions exploitation. *Water Environ. Res*. 79, 421–429.

Pellera, F. M., & Gidarakos, E. (2015). Effect of dried olive pomace – derived biochar on the mobility of cadmium and nickel in soil. *J. Environ. Chem. Eng*. 3, 1163–1176.

Rousidou, C. Papadopoulou, K. Zervakis, G. Singh, B. K. Ehaliotis, C. & Karpouzas, D. G. (2010). Repeated application of diluted olive mill wastewater induces changes in the structure of the soil microbial community. *European J. Soil Biol*. 46, 34–40.

Song, S. T., Hau, Y. F., Saman, N., Johari, K., Cheu, S. C., Kong, H., & Mat, H. (2016). Process analysis of mercury adsorption onto chemically modified rice straw in a fixed-bed adsorber. *J. Environ. Chem. Eng*. 4, 1685–1697.

Stasinakis, A. S., Elia, I., Petalas, A. V. & Halvadakis, C. P. (2008). Removal of total phenols from olive-mill wastewater using an agricultural by-product, olive pomace. *J. Hazard. Mater*. 160, 408–413.

Tamuly, C., Hazarika, M., Das, J., Bordoloi, M., Borah, D. J., & Das, M. R. (2014). Bio-derived CuO nanoparticles for the photocatalytic treatment of dyes. *Mater. Lett*.123, 202–205.

Yipmantin, A., Maldonado, H. J., Ly, M., Taulemesse, J. M., & Guibal, E. (2011). Pb(II) and Cd(II) biosorption on Chondracanthus chamissoi (a red alga). *J. Hazard. Mater*. 185, 922–929.

Zagklis, D. P., Vavouraki, A. I., Kornaros, M. E., & Paraskeva, C. A. (2015). Purification of olive mill wastewater phenols through membrane filtration and resin adsorption/desorption. *J. Hazard. Mater*. 285, 69–76.